Original paper

Long bone histomorphogenesis of the naked mole-rat: ontogeny, histodiversity and intraspecific variation

Germán Montoya-Sanhueza[1,2*], Nigel C. Bennett[3], Maria K. Oosthuizen[3], Christine M. Dengler-Crish[4], Anusuya Chinsamy[1]

[1]*Department of Biological Sciences, University of Cape Town, Private Bag X3, Rhodes Gift 7701, South Africa.*
[2]*Department of Zoology, Faculty of Science, University of South Bohemia, Branišovská 1760, České Budějovice 37005, Czech Republic.*
[3]*Mammal Research Institute, Department of Zoology and Entomology, University of Pretoria, Pretoria 0002, South Africa.*
[4]*Department of Pharmaceutical Sciences, Northeast Ohio Medical University, Rootstown, OH, USA.*

*Corresponding author: GM-S, getamoo@gmail.com

Keywords: Bone microstructure, Long bone growth, Bone modeling, Lamellar bone, Lamellar-zonal bone, Endosteal bone, *Heterocephalus glaber*.

Short running title: Bone microstructure of naked mole-rats

ABSTRACT

Lacking fur, living in eusocial colonies and having the longest lifespan of any rodent, makes naked mole-rats (NMRs) rather peculiar mammals. Although they exhibit a high degree of polymorphism, skeletal plasticity and are considered a novel model to assess the effects of delayed puberty on the skeletal system, scarce information on their morphogenesis exists. Here we examined a large ontogenetic sample (n = 76) of subordinate individuals to assess the pattern of bone growth and bone microstructure of fore- and hindlimb bones by using histomorphological techniques. Over 290 undecalcified thin cross-sections from the midshaft of the humerus, ulna, femur and tibia from pups, juveniles and adults were analyzed with polarized light microscopy. Similar to other fossorial mammals, NMRs exhibited a systematic cortical thickening of their long bones, which clearly indicates a conserved functional adaptation to withstand the mechanical strains imposed during digging, regardless of their chisel-tooth predominance. We describe a high histodiversity of bone matrices and the formation of secondary osteons in NMRs. The bones of pups are extremely thin-walled and grow by periosteal bone formation coupled with considerable expansion of the medullary cavity, a process probably tightly regulated and adapted to optimize the amount of minerals destined for skeletal development, to thus allow the female breeder to produce a higher number of pups, as well as several litters. Subsequent cortical thickening in juveniles involves high amounts of endosteal bone apposition, which contrasts with the bone modeling of other mammals where a periosteal predominance exists. Adults have bone matrices predominantly consisting of parallel-fibered bone and lamellar bone, which indicate intermediate to slow rates of osteogenesis, as well as the development of poorly vascularized lamellar-zonal tissues separated by lines of arrested growth (LAGs) and annuli. These features reflect the low metabolism, low body temperature and slow growth rates reported for this species, as well as indicate a cyclical pattern of osteogenesis. The presence of LAGs in captive individuals was striking and indicates that postnatal osteogenesis and its consequent cortical stratification most likely represents a plesiomorphic thermometabolic strategy among endotherms which has been suggested to be regulated by endogenous rhythms. However, the generalized presence of LAGs in this and other subterranean taxa in the wild, as well as recent investigations on variability of environmental conditions in burrow systems, supports the hypothesis that underground environments experience seasonal fluctuations that may influence the postnatal osteogenesis of animals by limiting the extension of burrow systems during the unfavorable dry seasons and therefore the finding of food resources. Additionally,

the intraspecific variation found in the formation of bone tissue matrices and vascularization suggested a high degree of developmental plasticity in NMRs, which may help explaining the polymorphism reported for this species. The results obtained here represent a valuable contribution to understanding the relationship of several aspects involved in the morphogenesis of the skeletal system of a mammal with extraordinary adaptations.

Abbreviations

CCCB	Compacted coarse cancellous bone
CL	Cement line
dTt	Distal origin of the third trochanter
ELB	Endosteal lamellar bone
HC	Haversian canal
HL	Howship's lacunae
LB	Lamellar bone
LZB	Lamellar-zonal bone
LAGs	Lines of arrested growth
MC	Medullary cavity
NC	Nutrient canal
NF	Nutrient foramen
NMR	Naked mole-rat
Os	Osteocytes
PFB	Parallel-fibered bone
PLB	Periosteal lamellar bone
PVC	Periosteal vascular canals
RC	Resorption cavity
RL	Resorption line
ShF	Sharpey's fibers
SO	Secondary osteons
Tr	Trabeculae
TrB	Trabecularized bone
VC	Vascular canal
WB	Woven bone
a	Anterior side
la	Lateral side
me	Medial side
p	Posterior side

1. INTRODUCTION

The subterranean naked mole-rat (NMR), *Heterocephalus glaber* is one of the most peculiar mammals in the world. They show a combination of unique traits such as the absence of fur, inability of maintaining a high and stable body temperature (i.e. poikilothermy) and a eusocial system with a marked reproductive skew (Jarvis, 1981; Buffenstein & Yahav, 1991). With a mean body mass of 33.9 g, they are the smallest species among African mole-rats (Jarvis & Sherman, 2002), although they can live for up to 30 years in captivity, thus having the longest lifespan of any rodent (Sherman & Jarvis, 2002; Dammann & Burda, 2007). In

comparison to other small terrestrial (surface-dwelling) mammals, NMRs also exhibit low basal body temperature, low metabolic rate, high thermal conductance and slow somatic growth rates (Buffenstein & Yahav, 1991; Bennett et al., 1991; O'Riain, 1996; O'Riain & Jarvis, 1998; Holtze et al., 2018; Šumbera, 2019). These, as well as other key features such as their tolerance to anoxia and cancer, low mortality rates, delayed puberty, neotenic traits (and pedomorphy), prolonged lifespan and non-dependent vitamin D mineral metabolism, have characterized the NMRs as a novel model for studies on biogerontology and biomedical research (e.g. Buffenstein et al., 1994; Bennett, 2009; Faulkes & Bennett, 2009; Edrey et al., 2011; Tian et al., 2013; Park et al., 2017; Skulachev et al., 2017; Ruby et al., 2018; Buffenstein et al., 2020; see also Braude et al., 2020).

Despite the wide range of studies focused on their ecology and physiology, there are only a few studies that have examined their skeletal system. Nevertheless, initial studies of their mineral metabolism contributed significantly to understanding some aspects of their skeletal homeostasis (Buffenstein, 2000). These studies reported generalized low levels of vitamin D3 metabolites (1,25-dihydroxyvitamin D3), thus suggesting NMRs showed a different regulation for the acquisition of calcium as compared to other mammals (Buffenstein et al. 1993, 1994). Instead, calcium is obtained by passive intestinal absorption, presumably via a non-saturable pathway (Pitcher et al. 1992; Buffenstein et al. 1993, 1994; Buffenstein & Pitcher, 1996). Based on studies on NMRs and other bathyergids, it was suggested that their teeth and bones could act as reservoirs of calcium, since increased skeletal depositions were observed after supplement of calcium and vitamin D (Skinner et al. 1991; Pitcher et al. 1994; Buffenstein et al. 1995; Buffenstein, 1996; Buffenstein & Pitcher, 1996). Therefore, a tolerance for vitamin D deficiency and an efficient mineral metabolism are also characteristic of NMRs. One of the most striking morphological adaptations of NMR are associated with the vertebral changes of the only reproductive female (queen) within the colony, which has significantly longer lumbar vertebrae for its body size compared to all other non-reproductive colony members (subordinates) (Jarvis et al., 1991; O'Riain et al., 2000; Dengler-Crish & Catania, 2007, 2009; Henry et al., 2007). Subordinates are suppressed from releasing sex steroid hormones due to the antagonistic behavior of the queen, which results in delayed puberty and therefore individuals live under a hypogonadic condition (Pinto et al., 2010). Several studies on humans and laboratory rodents have revealed that hypogonadism results in suboptimal skeletal development and may lead to an increased risk of bone fractures later in life (Golden & Carlson, 2008; Yingling & Taylor, 2008; Pinto et al., 2010). However, the

147 femur of NMRs maintains robust bone structure and mechanical properties for most of their
148 lifespan (e.g. Pinto et al., 2010; Carmeli-Ligati et al., 2019). This suggests a positive
149 imbalance in mineral metabolism with low levels of age-related bone loss during life (i.e.
150 reduced osteopenia). Similar pattern has been described for the long bones of the largest
151 bathyergid, the solitary Cape dune mole-rat, *Bathyergus suillus* (mean body mass of 1497.7
152 g, Montoya-Sanhueza & Chinsamy, 2017, 2018; Montoya-Sanhueza et al., 2019).
153 Nevertheless, these observations have been based on the analysis of femora predominantly
154 (Chinsamy & Hurum, 2006; Pinto et al., 2010; Carmeli-Ligati et al., 2019), so whether this
155 process represents a specific pattern of this particular bone or a generalized feature of the
156 appendicular system of NMRs is unknown. NMRs are primarily chisel-tooth diggers, so they
157 use their continuously growing extra-buccal and highly procumbent incisors to excavate
158 tunnels (Jarvis & Sale, 1971; Berkovitz & Faulkes, 2001). However, they also use their
159 forelimbs and hindlimbs for both tunnel excavation and soil transport (Jarvis & Sale, 1971;
160 Tucker, 1981), so that their limb bones also experience important strains during digging
161 behavior. Because of this, a systemic adaptation of their appendicular system to maximize
162 their bone structure would be expected.

163 In a recent study, Carmeli-Ligati et al. (2019) used multiple histomorphometric techniques,
164 including micro-CT scanning, scanning electron microscopy (SEM) and polarized light
165 microscopy to describe the bone microstructure of the femora, mandibles and lumbar
166 vertebrae of subordinate NMRs during ontogeny. They found that the cortical bone of NMRs
167 is entirely composed of lamellar bone (LB) at all ontogenetic stages (Carmeli-Ligati et al.,
168 2019), although this differs from earlier histological reports of NMRs also describing woven
169 (WB) and parallel-fibered bone (PFB) in both the femur and humerus (Chinsamy & Hurum,
170 2006; Montoya-Sanhueza & Chinsamy, 2016). Because these data appear contradictory a
171 multi-skeletal assessment of NMR's bone histology throughout ontogeny is strongly needed.

172 Additionally, the typology of bone tissue matrices in tetrapods has been traditionally
173 associated with rates of osteogenesis and rates of somatic growth, i.e. more disorganized bone
174 tissues like WB are typically associated with fast rates of bone formation, whilst more
175 organized configurations like LB with slow bone formation (Amprino, 1947; Smith, 1960;
176 Klevezal, 1996; de Margerie et al., 2004; Chinsamy-Turan, 2005), thus reflecting the general
177 growth pattern of the animal. In this sense, African mole-rats have lower somatic growth
178 rates as compared to surface-dwelling mammals of similar size (Bennett et al., 1991), as well
179 as having a wide diversity of thermoregulatory modes ranging from so-called poikilothermy

in NMRs through to a tendency to poikilothermy in some furred species, to endothermy in the remaining species (Bennett, 2009; Šumbera, 2019), whereby they have been denoted as a model for the evolution of endothermy (Bennett et al., 1991; Bennett, 2009). Due to their particular ecophysiology and metabolism, NMRs and other mole-rat species represent important animal models for our understanding of the physiological processes involved during skeletal morphogenesis, especially to understand how these features are reflected in their bone microstructure. Moreover, the study of the skeletal morphogenesis of these subterranean rodents may represent a unique opportunity to understand the morphological adaptations and growth strategies of extant small mammals and its relationship with the underground environment. In this study, we describe the bone microstructure of zeugopodial and stylopodial bones of a large sample of subordinate NMRs, specifically focusing on their bone matrix composition (histodiversity), changes during ontogeny, its distribution within the cortex, as well as their general pattern of bone growth (bone modeling).

2. MATERIAL AND METHODS

A total of 76 NMRs of both sexes were analyzed (Table 1). The sample includes non-reproductive (subordinate) individuals obtained from different colonies (Table 1). The sex of the individuals was assessed by visual inspection and following the methodology of Seney et al. (2009). Most specimens came from captive colonies kept at the University of Cape Town (UCT) by Emeritus Associate Prof. Jennifer Jarvis. These colonies have been relocated to the University of Pretoria (UP) under the care of Prof. Nigel Bennett (Table 1). The colonies are housed in Perspex artificial burrow systems and fed *ad libitum* with a mixture of vegetables, fruits and a balanced cereal, Pronutro (Bokomo, Malmesbury, South Africa). The colonies were housed at temperatures of 29-31°C, at ~40% humidity and with a 12L:12D light cycle (light: 07:00–19:00 h). Ten specimens of known-age came from colonies kept at Northeast Ohio Medical University (NOMU) by Prof. Christine Dengler-Crish (Table 1). These NMRs were maintained in colony rooms with ambient temperatures of ∼30 °C and 40-60% relative humidity. For complete housing details of these individuals see Artwohl et al. (2002). For further identification of the individuals, we used the last three numbers of their ID codes (Table 1). Ethical approval for specimens #507-511 was obtained from the Animal Ethics Committee of the UP (AEC–UP: EC024-17) and for the specimens #156-164 from the NEOMED Institutional Animal Care and Use Committee in accordance with the Guide for Care and Use of Laboratory Animals published by the National Institutes of Health.

213

214 ## 2.1 Ontogeny: Molar Eruption and Relative Stages

215 Based on the molar eruption and dental wear, we classified NMRs into pups, juveniles and
216 adults (Table 1). Pups have two molars erupted from alveolar bone, while juveniles and
217 adults showed three molars. The molars of pups showed little wear and the cuspids are clearly
218 visible. Juveniles were differentiated from adults by having reentrant folds of enamel (in-
219 folding), whereas adults had molars with simple enamel rings indicating advanced tooth wear
220 (Jarvis & Sherman, 2002). Previous reports state that pups may take 4-24 months to attain
221 adult body mass (BM) and after this period they decrease their growth rates or are no longer
222 growing (e.g. Jarvis et al. 1991; Pinto et al., 2010). Because the skulls of the specimens of
223 known-age (#155-164) were not available, they were not classified using dental features.
224 These specimens were older than two years and therefore they were considered as adults
225 (Table 1).

226 ## 2.2 Long Bone Histology

227 Detailed qualitative descriptions of the bone histology and microanatomy of stylopodial
228 (humerus and femur) and the largest zeugopodial (ulna and tibia) elements of each limb, from
229 mostly the left side, were used. Because the radius and fibula represent comparatively smaller
230 bones with small transversal sections as compared to their serial homologous (ulna and tibia,
231 respectively) (Montoya-Sanhueza, 2020), they were not included in this study. After
232 skeletonization of long bones, they were fixed in 96% ethanol for at least 48 hrs and followed
233 by immersion in acetone for 1-2 hrs prior to sectioning (Montoya-Sanhueza, 2014). Standard
234 undecalcified histological procedures followed Chinsamy & Raath (1992) and Montoya-
235 Sanhueza & Chinsamy (2017), and consisted of analyzing the midshaft of the diaphysis (i.e.
236 ~50% of the total bone length from the proximal articular surface). A total of 292 thin cross-
237 sections of ~80–100 μm thickness were obtained and high-quality photomicrographs were
238 taken using a Nikon Eclipse E200 Polarizing Microscope.

239 Bone tissues were visualized using conventional transmitted light and polarized light
240 microscopy with a gypsum (¼ lambda) filter. Bone types were identified based on shape of
241 osteocyte lacunae, pattern of bone apposition, orientation of the collagen fibers and degree of
242 vascularization, following the nomenclature of Enlow (1963), Francillon-Vieillot et al.
243 (1990), de Ricqlès et al. (1991), Bromage et al. (2003) and Chinsamy-Turan (2005, 2012).
244 Other sources used for the identification of bone tissue types were based on developmental
245 and ontogenetic studies (e.g. Goldman et al., 2003; McFarlin, 2006; Warshaw, 2008;

Montoya-Sanhueza & Chinsamy, 2017). For a more appropriate description of bone tissue distribution within the cortex, this was divided into three relatively proportional regions: endocortical, intracortical and pericortical (e.g. Allen & Burr, 2014: Montoya-Sanhueza & Chinsamy, 2017).

<Table 1>

3. RESULTS

Since the bones of the pup exhibited similar bone microstructure, these were briefly described together in the first section below. Subsequent descriptions encompass each bone element (humerus, ulna, femur and tibia) including the main ontogenetic features of juveniles and adults.

Pups

One pup (#010, 4 months old) was examined. Long bones showed relatively thin cortical walls and a large medullary cavity (MC). The cortex presented rounded osteocytes distributed in a disorganized fashion within the matrix, thus representing woven bone (WB) (Fig. 1A). The cross-sectional geometry (bone microanatomy) of the humerus and femur is ellipsoidal, and these resemble the generalized cross-sectional shape of adults, whilst the ulna and tibia have a less differentiated shape compared to the adult diaphyseal phenotype. In general, the lack of periosteal resorptive surfaces, indicates that periosteal bone formation occurs around the entire cross-section. However, a clear cortical drift was observed in the femur: there is a conspicuous mineralizing front on the posterior side, with profusion of enlarged periosteal vascular canals associated with the external surface (Fig. 1A-B), as well as Howship's lacunae indicating active endosteal resorption in the posterior side (Fig. 1C). The external morphology of the femur clearly shows high vascularization associated with the periosteum on the posterior side (next to the nutrient foramen), whereas the anterior side shows a more even surface lacking vascularization (Fig. 1B). These data indicated that the main growth direction of the femur during perinatal age occurs towards the posterior region. These enlarged periosteal vascular canals were associated with sites of muscle attachment, such as the tip of the third trochanter in the femur (Fig. 1B), as well as with the tip of the deltoid crest in the humerus (anterolateral side). The latter indicates that the main mineralizing front in the

humerus is towards the anterolateral side. The ulna and fibula did not show enlarged periosteal vascular canals, probably due to the lack of conspicuous sites for muscle attachment in the diaphysis of these bones.

<Figure 1>

Humerus

Juveniles. The cortical thickness of juveniles is highly variable (Fig. 2). This suggests that cortical thickness may increase during this stage. The smaller juveniles exhibited relatively larger bones (diameters) as compared to pups, although they still had thin cortical walls and a large MC, e.g. #046 vs #010 (Fig. 2A). The cortex of smaller juveniles is mostly composed of WB and parallel-fibered bone (PFB), this latter showing better organized osteocytes (Fig. 2D-F). Periosteal expansion seems to occur around all bone surfaces without evidence of strong cortical drift as seen in the pup. However, a conspicuous resorption line (RL) in the intracortical region reveals a change in osteogenic activity that occurred earlier in ontogeny (Fig. 2E). These data suggest a change from predominantly periosteal growth to endosteal bone apposition in the anterior side (Fig. 2E), while the lack of a RL in the posterior side (Fig. 2F) indicates continuation of periosteal bone formation, predominantly lamellar bone (LB). At this stage, the anterolateral side shows considerable intracortical and endosteal resorption, which results in the formation of trabeculae (trabecularized bone) (Fig. 2D). In larger juveniles, some trabeculae were also observed at the anterior side of the MC, developing from the endocortical region (Fig. 2B) and sometimes appearing isolated within the MC.

Larger juveniles showed considerable formation of endosteal lamellar bone (ELB), (e.g. #045, #067, Fig. 2B), indicating changes in bone tissue composition to a more organized bone matrix and therefore suggesting a slowing of the rates of osteogenesis. A layer of ELB often surrounds the MC (Fig. 2H). The anterolateral side also shows RCs, although secondary reconstruction and development of compacted coarse cancellous bone (CCCB) was also observed in this region (Fig. 2G). The posterior region maintained considerable amounts of subperiosteal WB, PFB and ELB (Fig. 2H), while lateral and medial sides were variable in cortical thickness and showed predominance of LB. Particularly, the lateral side showed PFB which changes to a more lamellar-zonal bone (LZB) in the posterolateral region. This LZB is

310 composed of intercalating bands of PFB/LB and thin layers of LB (annuli), thus indicating
311 periodic changes in the rates of bone apposition (Fig. 2H). Some regions of the pericortical
312 region showed decreased rates of osteogenesis evidenced by formation of periosteal LB
313 (PLB). Short radial vascular canals also developed in the compacta of some individuals,
314 especially around the posterolateral side, while the anterolateral side showed longitudinally
315 arranged canals. In the medial side (concave surface of the bone), scarce vascularization was
316 present and the cortex was relatively thinner than in the lateral side, usually with bone tissues
317 arranged in a "compressed" fashion.

318 ***Adults.*** Individuals have a more triangular and robust cross-sectional shape with thick
319 cortical walls (Fig. 2C). Larger individuals exhibited more elongated cross-sectional shapes
320 (anterolateral axis). The medial side remains slightly concave and the lateral side is even or
321 slightly convex.

322 The cortex is mostly composed of PFB and LB (in lateral, medial and posterior sides) (Fig.
323 2J), and the anterolateral side still showed more disorganized tissues like WB and CCCB
324 (Fig. 2I). Individuals also showed a variable level of trabecularization in the anterolateral
325 region (Fig. 2I), thus suggesting faster bone turnover for this region in comparison to the
326 other regions of the cortex throughout ontogeny. The anterolateral region also had an
327 irregular periosteal surface, with the presence of longitudinal canals and Sharpey's fibers,
328 these latter structures were also identified in the posteromedial side. Both WB and PFB can
329 show high lacunar density compared to LB matrices. LZB also appeared in the medial and
330 posterior sides. LAGs and annuli were also observed in the anterolateral and anteromedial
331 sides, as well as in the posterior side. RLs indicating cortical drift are mainly located in the
332 posteromedial side (Fig. 2J). These marks evidence a change in growth direction from
333 periosteal to endosteal in early ontogeny and the predominance of endosteal bone formation
334 in this region (Fig. 2H). Secondary osteons (SOs) were scarce, but present in a high number
335 of individuals (47.89%) (Fig. 2K). One of the specimens (#079) showed considerable
336 trabecularization of the anterolateral side, intracortical resorption in the posterior side and
337 secondary reconstruction. The bone microanatomy of this specimen also appeared slightly
338 altered, showing a more pronounced concavity in its medial side.

339 The humerus of the specimens of known-age (mean 2.58 years) was similar to the other
340 adults of this study. These specimens showed thick cortical walls and their cortices were
341 generally well-vascularized. The old specimen (~10 years, #008) showed increased endosteal

342 resorption and trabecularization of the anterolateral region, thus showing a larger medullary
343 cavity size compared to the smaller and younger adults (Fig. 2C). In this specimen, the
344 posterior side showed increased amounts of slowly deposited PLB (Fig. 2J).

345

346 <Figure 2.>
347

348 *Ulna*

349 ***Juveniles***. There is considerable variation in cortical thickness among individuals (Fig. 3A).
350 This bone exhibited a higher degree of occlusion of the MC than the humerus of the same
351 individual (e.g. #046 in Fig. 3A vs. Fig. 2A). This suggested that the ulna reached higher
352 bone compactness (i.e. peak bone mass) before the humerus, which are maintained during
353 ontogeny (e.g. #067 in Fig. 3A vs Fig. 2A). Some specimens already showed an adult
354 morphology with a cortex composed of several bone tissues including WB, PFB, LB and
355 LZB (Fig. 3C). The lateral (concave) side is mostly composed of WB, while the medial side
356 shows LZB including bands of PFB and thin layers of LB annuli that extend towards the
357 anteromedial region, and becomes a more organized PLB tissue in the pericortical region
358 (Fig. 3B). The anterior and posterior sides showed considerable thickening, usually composed
359 of a mixture of bone tissues (Fig. 3C). At this stage, a distinct band of WB delimited by RLs
360 appeared in the intracortical region of the posterior side, thus showing an earlier reversal in
361 the direction of bone formation, from periosteal to endosteal, although periosteal apposition
362 of slowly deposited tissues (PLB) also continued during ontogeny (Fig. 3C). LAGs and LB
363 annuli were observed in the anterior and posterior regions of the bone (Fig. 3B, C).

364 ***Adults***. All individuals showed similar teardrop-like cross-sectional shape, with thick cortical
365 walls and a small MC lacking trabeculae (Fig. 3A). Among all the bones studied, only the
366 ulna had a MC that tended to occlude almost completely in some individuals. For this reason,
367 this bone showed the highest levels of compactness among all bones analyzed. The cortex
368 was mostly composed of PFB, LB and LZB, although some patches/bands of WB were also
369 observed in the anterior and posterior sides (Fig. 3B, C). The intracortical bands of WB were
370 delimited by RLs that remained from earlier ontogenetic stages (Fig. 3C). This band
371 evidenced changes in the rates of bone formation, now showing slowly deposited bone tissues
372 in endocortical (ELB) and pericortical (PLB) regions, especially comprising the anterior and
373 posterior regions of the bone (Fig. 3C). The pericortical region of the anterior and posterior
374 sides is composed of slowly formed PLB. Sharpey's fibers were found in the pericortical

region of the anterior side, most likely associated with the interosseous ligament that connects the ulna with the radius. Only a few individuals (4.48%) showed SOs. The bones of adults exhibited quite scarce bone resorption, except one specimen (#079), which showed higher endosteal resorption and a slightly altered bone microanatomy, although less pronounced as compared to the humerus of the same individual. The histology of specimens of known-age (mean 2.58 years) was similar to other adults in this study. Apart from the increased bone size due to periosteal formation (Fig. 3C), no considerable changes in bone microstructure were detected for the specimen of ~10 years (#008).

<Figure 3>

Femur

Juveniles. The femur showed variable degrees of cortical thickness and the MCs also varied considerably in size (Fig. 4A, B). In small individuals, the cortex consisted of rapidly formed WB and PFB, lacking cortical vascularization (Fig. 4D-F). The cortex of larger juveniles was comprised of predominantly of PFB, LB and LZB in the posterior and lateral sides (Fig. 4G), whereas anterior sides showed mostly LB. Remnants of WB were found in several regions of the bone (Fig. 4G). The femur elongated mediolaterally, with its lateral side being quite sharp (Fig. 4G) and coinciding with the distal origin of the third trochanter, while the medial side was robust and rounded (Fig. 4H). Larger specimens showed conspicuous LZB consisting PFB and LB annuli, especially in the medial side of the cortex (Fig. 4H, I). As in the humerus, a distinct RL was detected in the intracortical region of the posterior side of larger individuals, thus indicating a clear shift in the direction of bone apposition during earlier ontogeny, from periosteal to endosteal (Fig. 4I). Signs of cortical drift such as the apposition of PLB in the posterior and lateral regions and resorption on their opposite sides, suggest that the growth of the femur continued towards the posterolateral side (Fig. 4I). LAGs were already observed in the tip of the lateral side (Fig. 4G, I, J), while annuli were mostly found in the medial side (Fig. 4H, I). At this stage, the humerus and femur of the same individuals have similar cross-sectional sizes (mediolateral diameter), although the femur appeared slightly smaller.

Adults. All specimens showed thick cortical walls and a relatively small MC (Fig. 4C). The MC generally lacked trabeculae, although some specimens developed them in the endocortical region and sometimes these appeared isolated within the MC. The lateral side

408 showed mostly PLB and PFB (Fig. 4J). Radial vascularization was evident in some
409 individuals in the anterior side (Fig. 4K) and a generalized low level of intracortical
410 resorption was observed. The cortex is composed primarily of subperiosteal PFB, especially
411 on the anterior side, although some LZB was observed in endocortical and pericortical
412 regions of the posterior side (Fig. 4L). For the same region of the cortex, some specimens
413 showed a variable predominance of either PFB, LB or LZB. RLs appeared in different
414 regions of the cortex, sometimes around the endocortical region, but also subperiosteally
415 (Fig. 4K, L). This indicated that the amount of endosteal bone was variable within the cortex
416 and among individuals, although often represented a high proportion of the cortex (Fig. 4K).
417 Bundles of Sharpey's fibers were associated with the periosteal margin of the posterior side.
418 Several individuals (12.16%) showed development of SOs. In comparison to the humerus, the
419 bone tissues of the femur were more evenly distributed and not so disorganized within the
420 cortex, indicating that the process of bone modeling was more uniform (isometric) around the
421 cortex, probably also associated with a slower bone turnover of this bone. This bone
422 exhibited limited bone resorption, although vascular canals were occasionally eroded. One of
423 the specimens (#079) showed considerable trabecularization of the MC, as well as
424 considerable secondary reconstruction.

425 The histology of specimens of known-age (mean 2.58 years) was similar to other adults in
426 this study, although the cortices of these specimens appeared generally well-vascularized.
427 Apart from the increased bone size due to periosteal bone formation, no considerable changes
428 in bone microstructure were detected for the specimen of ~10 years (#008, Fig. 4C, J-L). In
429 this specimen, the lateral side was composed of mostly PLB (Fig. 4J), while the anteromedial
430 side showed a very thin layer of PLB (Fig. 4K).

431

432 <Figure 4>
433

434 *Tibia*

435 ***Juveniles.*** There was a wide variation in cortical thickness and cross-sectional shape among
436 individuals (Fig. 5A). Small juveniles showed thin cortical walls and a large MC without
437 trabeculae, whilst larger juveniles showed thicker cortical walls with relatively small MCs
438 (Fig. 5A). The microanatomy of this bone was generally ellipsoidal. In the smaller juveniles,
439 the cortex was mostly composed of intercalations of WB and PFB, as well as some areas
440 showed apposition of LB. This stratification was more evident in larger juveniles, which

showed mostly PFB and LB forming LZB (Fig. 5B, C), as well as small patches/bands of WB. Annuli were found around the entire cross-section, including endocortical regions. No strong cortical drift was observed in this bone, thus indicating a relatively balanced radial growth in all directions. Almost no RCs were observed at this stage in this bone.

Adults. In general, the tibia had a variable shape in cross-section, from subcircular to triangular, with thick cortical walls and a relatively small MC with no trabeculae. During ontogeny, the amount of LB in the cortex increased considerably (Fig. 5D), although some remnants of WB were still observed (Fig. 5E). There was a clear differentiation between WB and LB tissues delimited by RLs (Fig. 5D). Similarly, a band of ELB could be found surrounded by a RL. CCCB was also observed in some specimens. Adults showed scarce bone resorption, sometimes with a MC completely occluded. This bone showed abundant lacunae, the presence of several LAGs, annuli and scarce vascularization, as well as only few individuals (5.63%) developed SOs. Only one specimen (#079) showed considerable trabecularization of the MC and secondary reconstruction with formation of SOs (similar to the femur of the same individual). The histology of specimens of known-age (mean 2.58 years) was similar to other adults in this study. Apart from the increased bone size, no considerable changes in general bone microstructure were detected in the specimen of ~10 years.

<Figure 5>

4. DISCUSSION

This study represents the first comprehensive assessment of the long bone histology and microanatomy of naked mole-rats (NMR). Different aspects of their histodiversity, matrix composition, cortical drift, growth and development are discussed here, primarily focusing on intraspecific variation, as well as on interspecific similarities and differences with other African mole-rats, rodents and fossorial mammals in general. In light of our large study sample, several misconceptions previously made on the bone growth and bone microstructure of NMRs are also revised.

Overall, the bone growth of the humerus, ulna, femur and tibia of NMRs is characterized by considerable cortical thickening, as well as reduced endosteal and intracortical bone resorption. Bone resorption (intracortical) was mostly restricted to the humerus, specifically

473 to the anterolateral region, where the muscles of the deltoid crest insert (Montoya-Sanhueza,
474 2020). Similar findings have been reported for the humerus of the largest bathyergid species,
475 the Cape dune mole-rat, *B. suillus*, which showed high intracortical resorption and high
476 vascularization just below the deltoid tuberosity, most likely due to the complex modeling
477 process of this bone due the humeral rotation and the relocation of the deltoid tuberosity
478 during ontogeny (Montoya-Sanhueza & Chinsamy, 2017; Montoya-Sanhueza, 2020).
479 Consequently, the humerus of NMRs (and most likely other bathyergids) exhibits a complex
480 pattern of bone modeling, high histodiversity and the highest levels of bone turnover among
481 the long bones analyzed. Among all the specimens analyzed only one specimen (#079)
482 showed extreme resorption of its cortices, i.e. endosteal bone resorption, trabecularization of
483 the medullary cavity and secondary reconstruction. Due to the generalized bone resorption of
484 this specimen, it is most likely that this process represents a systemic pathology affecting its
485 skeleton. Similar findings were reported for a subadult specimen of wild-caught Cape dune
486 mole-rats (Montoya-Sanhueza, 2014), thus indicating that disorders associated with mineral
487 imbalances are also present in wild and captive mole-rats. Additional analysis pertaining to
488 the extent and causes of the bone remodeling process of NMRs are needed to fully
489 understand their bone dynamics.

490 In general, the thick cortical walls found in the femur of adults (Fig. 4C) were similar to those
491 reported for the femur of this species in previous studies (Botha & Chinsamy, 2004;
492 Chinsamy & Hurum, 2006), which have shown statistically significant increments in cross-
493 sectional area, cortical area and thickness (Pinto et al., 2010; Carmeli-Ligati et al., 2019). Our
494 results demonstrate that the considerable cortical thickening of the femur, along with that
495 found in the humerus, ulna and tibia (Fig. 2C, 3A, 5A), represent a systemic pattern of bone
496 ossification. This pattern has also been reported in *B. suillus* and has been associated with an
497 adaptation to maximize the biomechanical properties of their bones to resist bending and
498 torsion strains during scratch-digging activities (Montoya-Sanhueza & Chinsamy, 2017).

499 Thus, the thick cortical walls observed in these African mole-rats (*H. glaber* and *B. suillus*)
500 represent an adaptation to their subterranean lifestyle, which are also concordant with the
501 reports of other subterranean rodents such as the tuco-tuco, *Ctenomys* (Ctenomyidae, Casinos
502 et al., 1993) and even larger fossorial mammals such as armadillos (Dasypodidae, Straehl et
503 al., 2013; Heck et al., 2019), the aardvark, *Orycteropus afer* (Orycteropodidae, Legendre &
504 Botha-Brink, 2018) and the common wombat (Vombatidae, *Vombatus ursinus*) (Walker et
505 al., 2020).

Our current knowledge on the bone microstructure of a wide range of fossorial taxa comprising a wide range of body sizes (from the small NMR to the large aardvark), as well as different social strategies (such as the solitary Cape dune mole-rat and the social NMR) have demonstrated a strong functional relationship between the morphology of long bones, ontogenetic cortical thickening and their specialization for digging behavior (Currey & Alexander, 1985; Biknevicius, 1993; Casinos et al., 1993; Montoya-Sanhueza *et al.,* 2019). These data evidence that NMRs, despite been predominantly chisel-tooth diggers (Jarvis & Sale, 1971; Tucker, 1981; Berkovitz & Faulkes, 2001), they still exhibit typical fossorial adaptations in their postcranial skeleton, indicating a highly conserved function of both fore- and hindlimbs for burrow excavation aiding either during scratch-digging, soil removal and/or for resisting their bodies while digging (e.g. Tucker, 1981; Samuels & Van Valkenburgh, 2008; Pinto et al., 2010). Future research should focus on the specific mechanisms of bone adaptation during the ontogeny of fossorial species, especially to understand the relationship between development and the onset of different biomechanical stimuli derived from locomotion in narrow spaces and digging behavior (e.g. Montoya-Sanhueza *et al.,* 2019).

Nonetheless, clear differences in the pattern of bone modeling are evident among fossorial taxa. Despite these taxa exhibiting thick cortical diaphyseal walls, their tissue composition, distribution and predominance within the cortex is variable, e.g. the cortical bone of NMRs is mostly composed of more lamellar configurations (see next section), while the cortex of *B. suillus* is composed of a mixture of bone matrices with varying degrees of fiber organization (Montoya-Sanhueza & Chinsamy, 2017). Similarly, the cortex of the aardvark *O. afer* is predominantly composed of bone of endosteal origin (Legendre & Botha-Brink, 2018). Such differences clearly reflect variations in the patterns of bone modeling, which are probably associated with different morphogenetic patterns (linked to body size differences), biomechanical functions and different life histories that are still poorly understood. This indicates that there is not a unique morphogenetic pathway to develop highly compacted bones in fossorial mammals and therefore that the factors influencing their bone modeling may be more varied than previously thought. Furthermore, among subterranean and fossorial mammals, the type of bone tissue they develop (or its architectural organization) is not correlated with their fossorial habits, so that the predominance of certain bone tissues should not be considered as indicators of digging activity.

539 ## 4.1 Bone tissue matrices and tissue configurations

540 The long bones of NMRs are composed of several bone tissue matrices, including woven
541 bone (WB), parallel-fibered bone (PFB) and lamellar bone (LB) (Fig. 1-5). Other
542 architectural configurations like compacted coarse cancellous bone (CCCB) and cyclical
543 bone tissue configurations such as lamellar-zonal bone (LZB) with annuli and lines of
544 arrested growth (LAGs) were also found (Fig. 1-5). In general, WB was present in all
545 specimens although only in pups it represented the main bone matrix, while PFB, LB and
546 LZB were predominantly found in juveniles and adults. Older ontogenetic stages showed
547 thicker bones with more organized bone matrices that are usually associated with lower rates
548 of osteogenesis in vertebrates (Amprino, 1947; de Ricqlès et al., 1991; Reid, 1996;
549 Chinsamy-Turan, 2005). In general, the postnatal morphogenesis of long bones of mammals
550 follows a relatively conserved pattern of bone matrix formation, from more rapidly formed
551 bone tissues (e.g. WB) to slowly formed bone tissues (e.g. LB) (Smith, 1960; Enlow, 1963;
552 Klevezal & Kleinenberg 1967; McFarlin, 2006; McFarlin et al., 2016; Chinsamy &
553 Warburton, 2020). Despite the wide variation of appositional rates found in bone tissue
554 matrices among vertebrates (e.g. de Margerie et al., 2002; 2004; Stark & Chinsamy, 2002),
555 this sequence is generally associated with the reduction in somatic growth rates observed
556 during ontogeny (Amprino, 1947; de Ricqlès et al., 1991; Castanet, 2006). In this sense, the
557 cortical bone growth of NMRs follows a similar pattern to other mammals showing high rates
558 of bone formation in early life and a subsequent decrease during adulthood. In a broad sense,
559 the bone histology and bone tissue organization of adult NMRs resembles that of lizards
560 (Squamata), which show avascular bone, a predominance of PFB in the inner cortical layers
561 and LB in the slow growing external cortex (Enlow, 1969; de Ricqlès et al., 1991). However,
562 considerable differences in the modeling process exist between these taxa which are probably
563 associated with the increased complexity of the bone modeling process acquired in mammals
564 (see next section).

565 This high histodiversity found in the long bones of NMRs has also been reported for other
566 bathyergids and fossorial mammals (Straehl et al., 2013; Montoya-Sanhueza & Chinsamy,
567 2017; Legendre & Botha-Brink, 2018; Heck et al., 2019; Montoya-Sanhueza, 2020), for
568 rodents in general (Foote, 1916; Ruth, 1953; Enlow & Brown, 1958; Enlow, 1962, 1963,
569 Singh et al., 1974; Francillon-Vieillot et al., 1990; de Ricqlès et al., 1991; García-Martínez et
570 al., 2011; Geiger et al., 2013; Orlandi-Oliveras et al., 2016) and for other larger eutherian
571 mammals such as primates, carnivores, ruminants and perissodactyls (Foote, 1916; Locke,

2004; Köhler et al., 2012; Marín-Moratalla et al., 2013; Kolb et al., 2015, Jordana et al., 2016, Nacarino-Meneses et al., 2016; Orlandi-Oliveras et al., 2018; Calderón et al., 2019, Becker et al., 2020, Smith, 2020). A high histodiversity in monotremes and marsupials has also been recently documented (Werning, 2013a; Walker et al., 2020; Chinsamy & Warburton, 2020). Therefore the histodiversity observed in the bone histology of NMRs does not differ considerably from that of other mammals.

However, the results of our study contrasts with previous histological assessments of long bones in NMRs, which were focused predominantly on the femur. The recent work of Carmeli-Ligati et al. (2019, p. 6, 11) reported that the femoral cortex of NMRs "*is composed entirely of circumferential lamellar bone, with sparse blood supply … and that they do not contain un-remodeled calcified cartilaginous islands*". Despite their wide ontogenetic sampling and the fact that they assessed both polarized light microscopy and SEM, these authors did not mention the presence of WB, PFB, LZB or CCCB. Based on a small sample size of the femur and humerus, Chinsamy & Hurum (2006) and Montoya-Sanhueza & Chinsamy (2016) reported WB, PFB and LB. Edrey et al. (2011) also briefly described some histological features, such as cortical and medullary cavity areas, LAGs, as well as growth plate and trabecular morphology, although they did not indicate the type of bone tissues.

In this study we did not detect islands of calcified cartilaginous tissue that result from the endosteal compaction or coalescence (Cadet et al., 2003) of trabecular (cancellous) bone at metaphyseal regions (Bach-Gansmo et al., 2013). This is most likely due to the small area that these regions occupy within the cortex (Bach-Gansmo et al., 2013). However, we detected CCCB, which is a common component of mammalian bone, also resulting from metaphyseal relocation and subsequent endosteal refilling, although its extension and amount within the diaphysis varies considerably during ontogeny and on the taxa (Enlow & Brown, 1958; Enlow, 1962, 1963; Montoya-Sanhueza & Chinsamy, 2017; Legendre & Botha-Brink, 2018; Heck et al., 2019). In NMRs, CCCB was found in several regions of the cortex, predominantly in the anterolateral region of the humerus and in the posterior region of the femur, usually associated with small patches of WB (e.g. Fig. 2G). It is likely that the small proportion of CCCB and WB, as well as the more organized nature of bone matrices in the femur of NMRs prevented its observation in previous studies. Because of the complex histology and bone modeling of the humerus, we suggest that further analysis of this element may be ideal to assess microstructural variability in this species.

604 Regarding the predominance of bone tissue matrices and its biological meaning in NMRs, a
605 previous study of an individual (most probably adult) from the same colonies kept at UCT
606 reported a richly vascularized region consisting of a more woven type of bone tissue, overlain
607 by a poorly vascularized outer circumferential layer (Chinsamy & Hurum, 2006). In our
608 wider sample, we observed that the long bones of juvenile and adult NMRs exhibited WB as
609 thin bands or patches distributed within the intracortical region (Fig. 2H, 3B), but never
610 covering extended surfaces of the cortex. Nevertheless, in pups and small juveniles, WB was
611 occasionally followed by transitional appositions of more organized tissues such as PFB with
612 rather rounded osteocyte lacunae, often covering a considerable area of the cortex (Fig. 2J).
613 Based on such findings, these latter researchers suggested that the earlier formed WB was
614 deposited at a faster rate than the outer more lamellar type of bone, and that this species
615 formed their bone tissues at a more rapid rate than that of many other extant small eutherians
616 such as moles, bats, marmots and squirrels (Chinsamy & Hurum, 2006), which tend to have
617 rather poorly vascularized compacta (Enlow & Brown, 1958). Here we suggest that this may
618 not be the case since the amount of WB in juvenile and adult NMRs is quite limited and the
619 ontogenetic bone histology and histodiversity of those small taxa is poorly known. For
620 example, Lee & Simons (2015) comprehensively described the bone histology of a
621 phylogenetically wide range of bat species, which exhibit long bones with thin cortical walls,
622 and reported the presence of three main bone matrices (WB, PFB and LB), thus indicating a
623 high histodiversity in these specialized mammals. This suggests that the bone microstructure
624 of small mammals, regardless of lifestyle, such as moles (subterranean), marmots (fossorial)
625 and squirrels (arboreal) may also record a more diverse histology during their life (Castanet,
626 2006). Further research must focus on the quantification of the rates of bone formation of
627 young NMRs, which have cortices composed of WB and PFB, as well as on comparing them
628 with other young small mammals, which also exhibit similar bone tissues during early
629 ontogeny.

630 An important component of the cortex of NMRs was LZB (Fig. 2H, 3C, 4H, 5C). This tissue
631 can be composed of LB or PFB with scarce vascularization and be organized in successive
632 depositional cycles, thus generally indicating quite slow and cyclical rates of bone deposition,
633 commonly found in reptiles (Francillon-Vieillot et al., 1990; Ricqlès et al., 2003; Chinsamy-
634 Turan, 2005; Köhler & Moyà-Solà, 2009). However, similar tissues have been reported in
635 other placentals and marsupials (Leahy, 1991; Chinsamy-Turan, 2005; Köhler & Moyà-Solà,
636 2009; Hurum & Chinsamy, 2012; Werning, 2013a, b). Recently, Chinsamy & Warburton

(2020) described the bone histology of femora and humeri of an ontogenetic series of western grey kangaroos (*Macropus fuliginosus*) and described zonal bone consisting of richly vascularized zones (fibrolamellar bone) and poorly vascularized annuli (PFB or LB). The cortical stratification of NMRs comprised of LB annuli and PFB zones represents a different bone tissue arrangement to that of the described marsupials and suggests comparatively slower bone growth rates. Among African mole-rats, the bone microstructure of NMRs exhibits the less vascularized cortices and a higher predominance of LB and LZB (Montoya-Sanhueza, 2020). Overall, the histomorphological analysis of NMRs and other African mole-rat species (Montoya-Sanhueza & Chinsamy, 2017; Montoya-Sanhueza, 2020) provides further insights into the relationship between bone growth rates and metabolism in mammals, suggesting that the more lamellar texture of the bones of subterranean mammals and some metatherians may reflect their generalized lower metabolic rates, lower body temperatures and slow somatic growth compared to eutherian mammals (McNab, 1966; Hulbert, 1980; Bennett et al., 1991; Zelová et al., 2007; Maloney et al. 2011; Šumbera, 2019), although it is important to consider that sampling biases in osteohistological studies have obscured the relevance of body size and phylogenetic signals in the understanding of mammalian bone growth patterns (Werning, 2013a, b).

4.2 Long Bone Growth and Bone Modeling

The cortical bone of juvenile and adult NMRs exhibited several RLs, usually located towards the external surface of the bone, in the pericortical and intracortical regions and which persisted throughout ontogeny (Fig. 2E, H, 3C, 4D, I). These RLs and other aspects of their cortical drift and perinatal morphogenesis suggest a different pattern of bone modeling in NMRs as compared to other mammals.

Long bones of mammals attain their peak bone mass either by augmenting bone density and/or bone size (Wall, 1983; Mora & Gilsanz, 2010). The first is positively correlated with cortical bone thickening (e.g. Webber et al., 2015), which results from intramembranous ossification throughout variable bone dynamics involving endosteal and periosteal bone formation (Smith, 1960; Enlow, 1963; Wall, 1983; Montoya-Sanhueza & Chinsamy, 2017), which is assumed to form the bulk of long bones (Smith, 1960; Hall, 1978; Wall, 1983). The second aspect, at least in terrestrial mammals, is the result of bone elongation (Mora & Gilsanz, 2010), which results from chondrocyte proliferation and bone matrix production

throughout endochondral ossification at growth plates (Kronenberg, 2003). Consequently, peak bone mass in long bones is attained by a dual process involving the interrelated modeling of endochondral and intramembranous ossification, which are known to have disparate genetic regulation (Beamer et al., 1996; Sanger et al., 2011; Wongdee et al., 2012). Most surface-dwelling mammals exhibit large medullary cavities with relatively thin cortical walls (Carrier, 1983; Heinrich et al., 1999; Lammers & German, 2002; Castanet, 2006; Young et al., 2010; Silva & Jepsen, 2013; Bala et al., 2015; Pazzaglia et al., 2015), mostly due to extensive endosteal bone resorption during ontogeny (Smith, 1960; Castanet, 2006). Similarly, surface-dwelling mammals seems to show more pronounced bone loss during ontogeny as a result of osteopenia, i.e. intrinsic age-related bone loss (e.g. Frost & Jee, 1992; Cerroni et al., 2000; Duque & Watanabe, 2011). For this reason, most of the bone growth observed during the process of bone modeling in medium to large mammals (except during infancy) is of a periosteal nature and/or from intracortical remodeling, while the endosteal component is considerably reduced or even completely obliterated by resorption (Smith, 1960; Enlow, 1962; Castanet et al. 2004, Castanet, 2006). This has been demonstrated by detailed quantifications of bone tissues in ruminants, primates and humans (e.g. McFarlin, 2006; Warshaw, 2008; Goldman et al. 2009; Cambra-Moo et al., 2014, 2015; McFarlin et al., 2016). Nevertheless, this does not mean that the cortex of such taxa do not contain endosteal tissues, but rather its proportion is relatively low and usually found around restricted areas of the perimedullary region. Evidence of these complex processes of periosteal and endosteal bone apposition are widely described by Smith (1960) and Enlow (1962, 1963), and can be histologically identified by the formation of reversal or resorption lines (RL). In most taxa, RLs are usually located in endocortical regions (subendosteally) thus suggesting a predominantly periosteal nature of the rest of the cortex (e.g. Enlow, 1962, 1963; Biewener & Bertram, 1993; Chinsamy-Turan, 2005; Chinsamy & Hurum, 2006). However, this pattern of bone modeling and predominance of periosteal growth contrasts with the observations made on NMRs.

The pups of NMRs tend to grow their skeletons primarily by formation of periosteal bone so that diametric expansion of cortical bone and simultaneous endosteal resorption occurs until juvenile stages (typical mammalian pattern). However, the diametric growth of the diaphysis of small juveniles appears relatively comparable in size to that of large juveniles and even to some small adults (Fig. 2A, B, 5A), thus indicating that the periosteal expansion of pups is constant through juvenile stages and soon after this they reach the adult size. This is also evidenced by the size of the medullary cavity area of pups and small juveniles, which appear

even larger than that of larger juveniles (Fig. 2A, B). At this point, the larger juveniles have similar cross-sectional areas to those of smaller juveniles, although thicker bones, thus indicating that endosteal bone formation has occurred and that periosteal bone formation has diminished their growth rates (reached plateau) during this transition. Despite the low sample size of pups and juveniles studied here, the young individuals analyzed by Carmeli-Ligati et al. (2019) showed similar trends, i.e. a microanatomy showing thin cortical walls.

The relevance of this process relies on the way that cortical thickening takes place. During this process, endosteal bone formation represents an important factor accounting for the attainment of peak bone mass in NMRs. This process is more evident in the humerus, ulna and femur, where single and/or double RLs are observed in the intracortical and pericortical regions of the bone separating the earlier formation of WB (in pups) from the subsequent apposition of more lamellar organization in juveniles and adults (Fig. 2H, 3C, 4I, K). These RLs indicate changes in the direction of bone apposition (from centrifugal to centripetal) and the more intracortical and pericortical location of these RLs suggest a higher predominance of bone tissues of endosteal origin (e.g. Chinsamy-Turan, 2005; Chinsamy & Hurum, 2006). Thus, the thin skeletal scaffold developed by pups and juveniles is in-filled with centripetal apposition of endosteally formed PFB and LB, thus providing the appropriate robustness to strengthen their bones (e.g. Fig. 2H). In the case of the tibia, this bone appeared to have a more balanced formation of endosteal and periosteal bone tissues. Further evidence supporting this model comes from previous quantification of microstructural parameters in NMRs. The fact that cortical thickness increased and MC area decreased during the juvenile-adult transition (between 0.5–3 and 3–10 years, Carmeli-Ligati et al., 2019) suggest the formation of endosteal bone. Based on similar quantitative microstructural parameters Pinto et al. (2010) mentioned that the femora of subordinates grow through subperiosteal expansion with no endocortical infilling or resorption occurring in the endosteal surface. This may be due to the fact these authors analyzed only adult individuals (older than 2 years), thus not including the transitional stages where cortical thickening occurs (this study). Consequently, peak bone mass in *H. glaber* is suggested to be attained initially by a relatively continuous periosteal bone apposition in pups and juveniles, and subsequently by considerable endosteal bone formation in older juveniles and adults. Overall, endosteal bone formation may represent an important process in the morphogenesis of the long bones of NMRs. Similar pattern has been found in the larger fossorial species, the aardvark (Legendre & Botha-Brink, 2018).

The scarce bone loss in long bones of adult NMRs suggests that osteopenia is quite limited, as also noted for the femur and other postcranial elements of this species (O'Connor et al., 2002; Pinto et al., 2010; Carmeli-Ligati et al., 2019), and recently for all bathyergid genera (Montoya-Sanhueza & Chinsamy, 2017; Montoya-Sanhueza, 2020). Carmeli-Ligati et al. (2019, *n* = 4) found that once the age of NMRs exceeds a period of 10 years the cross-sectional area significantly decreases, and the medullary cavity area increases mostly due to endosteal resorption. The femur of our specimen of ~10 years showed increased cross-sectional size mostly due to periosteal bone formation, although its medullary cavity size did not change in size compared to other adults (Fig. 4C). However, the medullary cavity of the humerus of the same individual appeared larger, thus indicating increased endosteal bone resorption and therefore suggesting interskeletal variation in mineral homeostasis among stylopodial bones (Fig. 2C).

Overall, this information suggests ontogenetic heterochrony of the intramembranous module (see Montoya-Sanhueza et al., 2019; Montoya-Sanhueza, 2020). Heterochronic patterns of periosteal and endosteal bone formation/resorption are known for humans and laboratory rodents, where periosteal/endosteal bone formation have a gender-based component, i.e. periosteal bone formation is greater in men than in women, and a greater part of the mid-diaphyseal cortex of women is of endosteal origin due to estrogen stimulation (Seeman, 2001; 2002). In developmental terms, the amounts of periosteal and endosteal bone formation during infancy are similar in primates (for femur) and these proportions change to a more periosteal bone predominance in adulthood (McFarlin et al., 2016). This may indicate that the synchronized and balanced activity of both endosteal and periosteal bone envelopes in some mammals may be characteristic of early postnatal stages and therefore may represent a pedomorphic condition. Whether these ontogenetic patterns represent a generality among mammals and whether NMRs retain a more pedomorphic growth it remains unknown and further quantification of their bone growth trends are needed to elucidate these questions.

4.3 Intraspecific variation: differential growth rates among subordinates

We identified several specimens of similar size and relative age showing variation in their matrix composition, i.e. some showed a cortex composed of more PFB configuration, whereas others showed a more LB or lamellar-zonal arrangement, thus indicating that bone

modeling and skeletal development occurred at different growth rates. This may indicate morphogenetic plasticity in NMRs, i.e. similar adult body sizes may be attained by differences in their relative rates of bone growth. Previous studies have already reported a considerable degree of phenotypic plasticity associated with the lumbar elongation of the females when achieving reproductive status (O'Riain et al., 2000; Henry et al., 2007; Dengler-Crish & Catania, 2007). In subordinates, a high intra-colony polymorphism in body size has been reported, which is usually associated with differential growth rates among individuals (Jarvis et al., 1991; O'Riain, 1996). O'Riain & Jarvis (1998) suggested that such plasticity in growth is the product of different ontogenetic histories (behaviors) of colony members that may serve as the basis for variation in size among adults. Similarly, the division of labor (polyethism) among subordinates, which allow individuals to form an effective workforce (e.g. Lacey & Sherman, 1991), may also represent a possible explanation for this process, although evidence supporting this phenomenon has been equivocal (see Gilbert et al., 2020). In any case, our preliminary results provide further support for the existence of morphogenetic plasticity among subordinate NMRs, which may help explain the tissue-level mechanisms involved in the generation of high intra-colony polymorphism as a product of differential bone growth rates. Is possible that the different behaviors within colony members (including ontogenetic polyethism), as well as the interaction of other social and environmental factors (e.g. Gilbert et al., 2020) may represent important factors to consider on further research assessing the bone growth of subordinates. Similarly, the fact that our specimens come from different colonies may have contributed to the high levels of polymorphism observed.

4.4 Cortical vascularization and secondary osteons

Bone vascularization was limited to a few radial (usually short and small) and longitudinal vascular canals, predominantly found in the cortex of the stylopods (humerus and femur) (Fig. 2G, 2I, 4K). The ulna and tibia showed considerably lower levels of vascularization. Nevertheless, vascularization was also variable among individuals, with some individuals showing several canals and others showing no vascularization at all. This is probably associated with the variability of bone tissue matrices and the high developmental plasticity found in this species (see previous section). Previous reports have described richly vascularized regions surrounding the medullary cavity and in which occasionally enlarged erosion cavities lacking osteonal development also occurred (Chinsamy & Hurum, 2006).

802 However, despite the considerable intraspecific variation in the pattern of vascularization in
803 NMRs, none of the specimens in the current study showed richly vascularized bone cortices.
804 In fact, recent quantifications of vascular density in the femur of NMRs have showed much
805 lower levels compared to other small rodents (Carmeli-Ligati et al., 2019). These
806 quantifications also showed non-significant differences for blood vessel density during
807 ontogeny (Carmeli-Ligati et al., 2019), although this may be obscured by the high vascular
808 variability reported here.

809 Bone resorption and secondary reconstruction (remodeling) of vascular canals was observed,
810 although rarely forming secondary osteons (= Haversian systems) (Fig. 2K). Nevertheless,
811 this is the first study to describe the presence of SOs in NMRs. These were present in almost
812 half of the individuals analyzed and mostly found in the humerus and femur, although in low
813 numbers (generally 1-2 per bone section). As previously noted for rodents (Ruth, 1953;
814 Enlow, 1962; Montoya-Sanhueza & Chinsamy, 2017), no Haversian bone (i.e. dense
815 aggregations of secondary osteons covering bone surfaces) was found in NMRs.

816 There have been previous confusing reports concerning secondary osteons in NMRs, either
817 reporting abundant secondary osteons and high bone remodeling (e.g. Buffenstein, 2008;
818 Edrey et al., 2011) or a complete lack thereof (Currey et al., 2017; Carmeli-Ligati et al.,
819 2019). Buffenstein (2008) mentioned the presence of many secondary osteons and high bone
820 remodeling, although no histological evidence was provided to support this. Chinsamy &
821 Hurum (2006) described enlarged erosion cavities in the compacta, although they lacked
822 osteonal development. In a subsequent study, Edrey et al. (2011) mentioned that there is
823 considerable variability in osteon number and size in NMRs. In respect to this latter study,
824 Carmeli-Ligati et al. (2019, p. 2) commented that "…*they base this conclusion on the*
825 *observation of a few round objects in transverse sections of the femoral diaphysis, but these*
826 *appear to us to be either primary osteons or blood vessels, and thus do not indicate*
827 *remodeling.*" We concur with Carmeli-Ligati et al. (2019) in that those structures do not
828 represent SOs and we suggest that such structures are probably (eroded) longitudinal canals,
829 as observed in some specimens in this study (Fig. 2G). On the other hand, Carmeli-Ligati et
830 al. (2019) mentioned the complete lack of osteons and therefore no bone remodeling in the
831 cortex of a large ontogenetic sample of NMRs. Based on the findings of the present study, we
832 reject the claims that *H. glaber* possess many secondary osteons or none.

The secondary osteons identified in NMRs were relatively small, highly irregular in shape and their cement lines were not always well-defined around their margins, making its identification difficult (Fig. 2K). Recently, Montoya-Sanhueza & Chinsamy (2017) and Montoya-Sanhueza (2020) reported SOs for all other bathyergid genera, whose species are larger compared to NMRs and their SOs appeared larger in size and more defined than in NMRs. A recent study revealed that larger mammals have larger osteonal and Haversian canal areas compared to smaller mammalian species in absolute terms, although these parameters are smaller in larger mammals and scale with negative allometry in relative terms (Felder et al., 2017). These authors suggested that osteonal development may represent a restricted or reduced process in smaller mammal species to avoid increased fracture risks (Felder et al., 2017). Whether NMRs and other African mole-rats follow a similar allometric pattern is unknown and further quantification is required.

4.5 Growth marks and cyclical growth

NMRs exhibited several bone tissues evidencing cyclical growth, including lamellar-zonal bone (PFB/LB with LB annuli) and lines of arrested growth (LAGs). Annuli (Fig. 2H, Fig. 4H) and LAGs (Fig. 3B) were observed within the PFB and LB matrices, and these indicate low rates of osteogenesis (annuli) or its complete growth cessation (LAGs) (Klevezal & Kleinenberg 1967; Castanet et al., 1993, 2004; Klevezal, 1996; Chinsamy-Turan, 2005; Castanet, 2006). In the case of annuli, these were composed of thin layers of LB developed during juvenile and adult stages. This stratification resulted in lamellar-zonal bone (LZB) that showed periods of relatively fast and slow bone formation, although not all individuals showed a clear stratification (see below). The high amount of bone tissues of lamellar nature is most likely a reflection of their low metabolic rates and body temperatures (Bennett & Faulkes, 2000). Whether NMRs have significantly lower metabolic rates and body temperatures as compared to other bathyergids is still under debate and additional investigations are needed to answer this question (see Šumbera, 2019). Nevertheless, the typology of the bone tissues of NMRs suggests that their skeletal growth may be slower compared to other bathyergids. In this respect, Montoya-Sanhueza (2020) analyzed the growth trajectories of the ossification patterns (endochondral and intramembranous) of long bones of all African mole-rat genera and detected the slowest growth rates to occur in NMRs. It has also been reported that the somatic growth rates of young NMRs are slower compared to other bathyergids, as well as to other surface-dwelling eutherians of similar size (O'Riain, 1996; O'Riain & Jarvis, 1998; Bennett & Faulkes, 2000; Buffenstein et al., 2020).

It is noteworthy that the cyclical bone growth observed in NMRs is different to that of other African mole-rats (Montoya-Sanhueza & Chinsamy, 2017; Montoya-Sanhueza, 2020) and mammals in general (Chinsamy-Turan, 2005; Kolb et al., 2015; Chinsamy & Warburton, 2020). This is because adult NMRs have bone cortices composed of more organized and slowly deposited bone tissues with predominantly lamellar components (e.g. PFB, LB), as well as less vascularization, so that the stratification appears less marked as compared to larger mammals which have clear alternations of vascularized and avascular bone tissues (e.g. Köhler & Moyà-Solà, 2009; Köhler et al., 2012; Jordana et al., 2016; Chinsamy & Warburton, 2020). Several factors have been associated with the formation of zonal bone in vertebrates including cyclic periods of hibernation, seasonal thermoregulatory fluctuations (heterothermy) and marked seasonal changes in feeding habits (e.g. Enlow, 1969; Köhler & Moyà-Solà, 2009; Köhler et al., 2012; Chinsamy & Warburton, 2020). The pattern described here for NMRs comprising a large sample of captive individuals is not easily attributable to environmental factors and therefore further elaboration to explain this pattern is required.

In the present study, we found LAGs in some captive NMRs, but not in all individuals. Although LAGs have typically been used for skeletochronological assessments in mammals (Castanet et al., 1993; Klevezal, 1996; Castanet, 2006), the relationship between the number of LAGs and age in the specimens of known-age of our study was not clear. In general, the LAGs were mostly evident on the anterior side of the ulna and lateral tip of the femur (e.g. Fig. 3B; Fig. 4J). The humerus also showed LAGs in different regions of the cortex, mainly in the posterior region, as well as in anterolateral and anteromedial sides. Due to the complex bone modeling of these bones, especially the humerus and ulna, it was not always possible to follow LAGs around the entire cross-section. However, the minimal cortical drift observed in the tibia allowed the observation of annuli around most of the cross-section. Some LAGs occurred endosteally (Fig. 2H), which have also been described in other mammals such as the gibbon, *Hylobates* (Klevezal, 1996). Additional studies in NMRs are needed to determine the specific patterns of LAG formation and age of the individual.

Edrey et al. (2011) also described LAGs in the lateral tip of the femur of NMRs, although they inadvertently associated such growth marks with fast growth patterns. Chinsamy & Hurum (2006) reported and illustrated the lack of LAGs in one specimen of *H. glaber*, suggesting that this could be because the animal was from a captive colony, so would not have endured seasonal environmental fluctuations and that this may also occur in the wild, since they live in burrows that experience minimal ambient fluctuations. In general, the

ambient temperatures of subterranean environments are considered more stable, with a lower magnitude of change over time (daily and seasonal) compared to above-ground environments (Bennett et al., 1988). However, based on recent studies, we actually know that the temperature of NMR's burrows in their environments in tropical regions (Ethiopia and Kenya) have wider fluctuations than previously thought (24.6–48.8°C), regularly alternating during day and night (Holtze et al., 2018). Thus, these environments still undergo daily and seasonal fluctuations and are especially greater in range at temperate latitudes (e.g. Bennett et al., 1988; Šumbera et al. 2004). This suggests that the underground environments also undergo fluctuations that may influence the pattern of osteogenesis of subterranean mammals. Indeed, LAGs have also been reported in bones of wild subterranean mammals: i) all long bones of wild-captured Cape dune mole-rats, *B. suillus* (Montoya-Sanhueza & Chinsamy, 2017); ii) mandibular periosteal bone of the greater molerat, *Spalax microphthalmus* (Spalacidae) (Hamar & Prodanascu, 1971; Puzachenko, 1991); and the iii) talpid mole, *Talpa europaea* (Kiselev, 1970, *fide in* Klevezal, 1996).

It is known that subterranean animals including some bathyergids undergo seasonal and daily thermoregulatory variations (Moshkin et al., 2001; Boyles et al., 2011; Streicher et al, 2011, Zelová et al. 2011; Lövy et al. 2013; Šumbera, 2019). Bathyergid species living in sub-tropical regions such as *Bathyergus*, *Georychus* and *Cryptomys* also show marked seasonal responses in breeding patterns compared to species living in equatorial regions such as NMRs (Lovegrove et al., 1993). This suggests that the daily and seasonal thermoregulatory and metabolic variations of subterranean mammals could have an effect on the formation of growth marks. Accordingly, the pattern of osteogenesis of the largest bathyergid *B. suillus,* appeared markedly stratified (Montoya-Sanhueza et al., 2017), probably reflecting the strong seasonality that this species experiences in temperate environments (Hart et al., 2006). However, this species exhibited a non-heterothermic pattern in the wild (i.e. no marked fluctuations of body temperatures was observed during the year) (Okrouhlík et al., *in press*), so the fluctuations in ossification rates documented for this species are probably linked to other environmental factors (see below). Among African mole-rats, NMRs exhibit poor thermoregulatory capabilities, especially the subordinates, which regulate body temperature over a narrow range of ambient conditions, outside of which pronounced thermolability is evident and they thermoconform to their environment (Buffenstein & Yahav, 1991; Hislop & Buffenstein, 1994; Woodley & Buffenstein, 2002; Buffenstein et al., 2020). Nevertheless, the study of Holtze et al. (2018) showed that the skin temperature of wild NMRs remained lower

than soil surface and burrow temperatures but did parallel the daily rise and fall in the burrow. These studies demonstrate that, in the wild, NMRs maintain functional body temperatures within the metabolically optimal range despite large fluctuations in daily ambient temperature (Holtze et al., 2018). For this reason, it appears that the pattern of cyclic osteogenesis observed in NMRs could be hardly associated with fluctuations of burrow temperature in the wild, which would be also true for the case of individuals in captivity. The development of growth marks in animals raised in captivity with constant ambient temperatures has also been reported in small primates (*Microcebus murinus*) (Castanet et al., 2004).

Food availability is proposed as another potential factor explaining the development of zonal bone in mammals (Klevezal, 1996; Köhler & Moyà-Solà, 2009). Foraging in wild NMRs is severely restricted during the dry season (Brett, 1991), which affects the hardness of the soil for tunnel excavation, consequently having seasonal energetic implications. In fact, the metabolic rate of NMRs is known to decrease by 25% when food is restricted for a period of 16 days (Goldman et al. 1999). Since food supply in the wild is more difficult to acquire during the dry season, this represents a potential factor influencing cyclical growth in NMRs and *B. suillus*. Still, food availability in captivity is unlimited.

Consequently, no evident link between cyclical growth and environmental fluctuation is detected in NMRs. It is possible that NMRs undergo intrinsic physiological fluctuations associated with annual rhythms, thus leaving a record during their postnatal osteogenesis. NMRs exhibit daily rhythms associated with their locomotor activity (Riccio & Godlman, 2000) and apparently also daily fluctuations in body temperature (Holtze et al., 2018), although no data on annual patterns have been reported for this species or the lengths of circannual rhythms to various zeitgebers. In general, circadian rhythms in above-ground animals are synchronized by day length, thus helping in the regulation of seasonal adaptations (Riccio & Godlman, 2000) and thus representing potential seasonal clocks for timing the onset of seasonal transitions in reproduction, metabolism and behavior (Ratajczak et al., 1993; Prendergast et al., 2004). Circannual clocks and seasonal interval timers have a strong genetic basis, so that their evolution and selection may play important roles on determining patterns of seasonality (Prendergast et al., 2004), as well as be responsible for the pace of bone development (Bromage et al., 2009). However, further studies assessing seasonal changes in NMRs are required to understand what kind of long-term fluctuations, if any, this species experience.

Overall, this information rather supports recent investigations suggesting that the periodicity of bone formation in vertebrates is the result of endogenous rhythms, which are associated with seasonal fluctuations of their metabolic rates, thermoregulatory strategies (e.g. heterothermy), hormonal activity and photoperiod, which are synchronized and/or reinforced by environmental cycles (seasonality) and/or availability of food resources (e.g. Klevezal & Mina, 1973; Klevezal, 1996; Castanet et al., 1993; 2004; Castanet, 2006; Köhler & Moyà-Solà, 2009; Köhler et al., 2012; Chinsamy & Warburton, 2020). In this sense, Köhler et al. (2012) suggested that cyclical growth is a universal trait of homoeothermic endotherms and that the arrested growth observed during unfavorable seasons in endotherms may arise as part of a plesiomorphic thermometabolic strategy for energy conservation. Thus, the pattern of cortical stratification of NMRs may be a reflection of a historically conserved endogenous rhythm, which appears less influenced by environmental fluctuations, food limitations and/or seasonality due to their life in captivity. Further analysis should focus on exploring how environmental and potential endogenous rhythms affect the growth patterns of wild and captive NMRs.

4.6 Pup Development and Reproduction in Naked Mole-Rats

The extremely thin cortical bone walls and large medullary cavity sizes observed in all long bones of the ~4 months old pup (Fig. 1) were unexpected for a highly fossorial species. However, similar bone microanatomy with thin cortical walls was previously reported for the femur of pups (<3 months old) of this species (Carmeli-Ligati et al., 2019). The juveniles of *B. suillus* also showed thin cortical walls (Montoya-Sanhueza & Chinsamy, 2017; Montoya-Sanhueza et al., 2019). It is probable that a generalized growth pattern occurs among African mole-rats and probably other fossorial species, where animals gradually thicken their long bones during postnatal ontogeny (i.e. cortical thickness would show positive allometry during ontogeny).

Although some authors have proposed rapid skeletal mineralization for young NMRs (e.g. Hood et al., 2014), this is clearly not reflected in higher accumulations of bone and/or cortical thickening at perinatal stages. Since the thin cortical walls of pups are composed of WB (Fig. 1), a bone tissue typically observed in mammalian neonates (Enlow, 1962, 1963) and associated with rapid osteogenesis (Francillon-Vieillot et al. 1990; de Ricqlès 1991), we suggest that the pups of NMRs have a pattern of bone modeling involving synchronized

997 periosteal bone formation and endosteal resorption to reach large somatic sizes (although
998 evidently compromising their bone robustness). This pattern of cortical growth is probably
999 related to the developmental and reproductive strategy of NMRs. The reproductive strategy
1000 of mammalian females usually involves highly demanding energetic processes (Oftedal,
1001 1980). Female breeders of NMRs have a long gestation period and slow postnatal
1002 development compared to other bathyergids (Bennett et al., 1991). Furthermore, the NMR
1003 has large average litter sizes (i.e. up to 27 pups in captivity) and the ability to produce several
1004 litters per year (Jarvis, 1991). Thus, reproduction in NMRs is associated with considerable
1005 somatic changes and increased metabolic rates in female breeders (Urison & Buffenstein,
1006 1994, 1995; Dengler-Crish & Catania, 2009; Šumbera, 2019). The pups are born relatively
1007 altricial (O'Riain, 1996), which has been proposed as a mechanism that enables the breeding
1008 female to generate larger litters (O'Riain, 1996). Our results on the skeletal anatomy of pups,
1009 further supports this hypothesis by demonstrating that pups receive minimal, but apparently
1010 sufficient amounts of minerals throughout lactation to primarily ensure postnatal
1011 morphogenesis and basic microstructural scaffolding of their skeletons. This process
1012 represents a compromise between the need to conserve the resources of the female during
1013 reproduction and the need to maintain nutrient intake of the young at a level that permits their
1014 optimal growth and development (Oftedal, 1980). Thus, the pups by developing their
1015 skeletons in size (rather than in bone mass) optimize the economy of the entire colony,
1016 mainly by directing small, but equal (low-dosage) amounts of resources to a larger number of
1017 newborns until they are able to feed more on solids and start autocoprophagy.

1018

1019 5. CONCLUSIONS

1020 Although *H. glaber* is primarily a chisel-tooth digger, its appendicular skeleton exhibited a
1021 systemic pattern of cortical thickening. This adaptation, which maintains relatively intact
1022 bone microstructure throughout ontogeny, evidences a conserved function of both fore- and
1023 hindlimbs to aid during burrow construction and foraging. The bone growth followed a
1024 typical pattern where individuals grew initially at a high rate and later turned to a slower
1025 growth pattern. The predominantly more organized bone matrices and scarce vascularization
1026 of NMRs indicate generalized low skeletal growth rates, most likely associated with the low
1027 metabolism, low body temperature and slow growth rates of this species. Despite this, the
1028 long bones of NMRs still exhibited high histodiversity, just as other mammals do. Likewise,
1029 despite the scarcity of secondary osteons in NMRs, this represents clear evidence of bone

remodeling. The study of the bone modeling of NMRs also evidenced a particular mechanism of cortical thickening where endosteal bone formation represents an important component of their long bones (and therefore periosteal bone formation is not solely responsible for the attainment of peak bone mass). Moreover, the early postnatal development of NMR's skeleton may be highly constrained by the extreme reproductive strategy of the female breeder, mostly to optimize mineral resources to ensure the appropriate development of many pups and consecutive litters. The presence of stratified cortices (LZB and LAGs) indicated the presence of cyclical patterns of bone formation in NMRs from captive colonies, thus probably associated with endogenous rhythms, although additional studies are needed to fully understand the proximate causes of this growth pattern. The variation in somatic growth previously reported for this species seems to be related to the developmental plasticity found in the rates of cortical formation among individuals.

ACKNOWLEDGEMENTS

We thank Marcelo Sánchez-Villagra (Universität Zürich) for his support during the completion of this study and Jennifer Jarvis for kindly granting us access to the specimens. We thank to two anonymous reviewers for their comments, which greatly improved the quality of this manuscript. GMS was supported by Becas Chile, the Government of Chile (CONICYT, 72160463). AC acknowledges funding from the National Research Foundation (NRF) no. 117716 (South Africa). NCB acknowledges funding from the SARChI chair of Mammalian Behavioural Ecology and Physiology from the DST-NRF South Africa (no. 64756). The research was cleared by the ethics committee of the University of Pretoria.

Author contribution

GMS and AC designed the study; AC supervised GMS's doctoral thesis and supported the experimental procedures; NB supported the experimental procedures; NB and CDC provided NMR specimens; MO and GMS quantified data and carried out bone labeling procedures; GMS, analyzed data, prepared the manuscript, created figures, acquired microscopy images; all authors made revisions to the original manuscript.

Declaration of competing interest

The authors declare no conflict of interest.

References

Allen M, Burr D. 2014. Bone Modeling and Remodeling (Ch. 4). In: *Basic and Applied Bone Biology* (Eds DB Burr, M Allen), pp. 373. Academic Press, Elsevier, London.

Amprino R. 1947. La structure du tissu osseux envisagée comme expression de différences dans la vitesse de l'accroissement. Arch Biol 58:315–330.

Artwohl J, Hill T, Comer C, Park T. 2002. Naked mole-rats: unique opportunities and husbandry challenges. Lab Anim.; 148:185–189.

Bach-Gansmo, F.L., S.C. Irvine, A. Brüel, J.S. Thomsen, H. Birkedal. 2013 Calcified cartilage islands in rat cortical bone. Calcif. Tissue Int. 92: 330–338.

Bala Y, Zebaze R, Seeman E. 2015. Role of cortical bone in bone fragility. Curr Opin Rheumatol 27: 406–413.

Beamer W, Donahue L, Rosen C, Baylink D. 1996. Genetic Variability in Adult Bone Density Among Inbred Strains of Mice. Bone 18: 397–403.

Becker, M, Witzel, C, Kierdorf, U, Frölich, K, Kierdorf, H. 2020. Ontogenetic changes of tissue compartmentalization and bone type distribution in the humerus of Soay sheep. J. Anat.; 237: 334– 354.

Bennett NC, 2009. African mole-rats (family Bathyergidae): models for studies in animal physiology. *Afr Zool*, 44:263–270.

Bennett NC, Faulkes CG. 2000. African Mole Rats: Ecology and Eusociality. Cambridge, UK: Cambridge University Press.

Bennett NC, Jarvis J, Aguilar GH, Mcdaid EJ. 1991. Growth and development in six species of African mole-rats (Rodentia: Bathyergidae). Journal of Zoology 225: 13–26.

Bennett, N.C., Jarvis, J.U.M., Davies, K.C., 1988. Daily and seasonal temperatures in the burrows of African rodent moles. South Afr. J. Zool. 23, 189–195.

Biewener AA, Bertram JEA. 1993. Mechanical loading and bone growth In Vivo. In: Bone Volumen 7 Bone Growth - B (ed BK Hall), pp. 353. CRC Press, Boca Raton.

Biknevicius, A. 1993. Biomechanical scaling of limb bones and differential limb use in caviomorph rodents. Journal of Mammalogy 74:95–107.

Botha J, Chinsamy A. 2004. Growth and life habits of the Triassic cynodont *Trirachodon*, inferred from bone histology. Acta Palaeontologica Polonica, 49: 619–627.

Boyles, J.G., Verburgt, L., McKechnie, A.E., Bennett, N.C., 2012. Heterothermy in two mole-rat species subjected to interacting thermoregulatory challenges. J. Exp. Zool. Part Ecol. Genet. Physiol. 317, 73–82.

Braude, S., Holtze, S., Begall, S., Brenmoehl, J., Burda, H., Dammann, P., del Marmol, D., Gorshkova, E., Henning, Y., Hoeflich, A., Höhn, A., Jung, T., Hamo, D., Sahm, A., Shebzukhov, Y., Šumbera, R., Miwa, S., Vyssokikh, M.Y., von Zglinicki, T., Averina, O. and Hildebrandt, T.B. 2020. Surprisingly long survival of premature conclusions about naked mole-rat biology. Biol Rev. doi: 10.1111/brv.12660

Brett, R.A., 1991. The ecology of naked-mole-rat colonies: burrowing, food, and limiting factors. In: Sherman, P.W., Jarvis, J.U.M., Alexander, R.D. (Eds.), The Biology of the Naked Mole-Rat. Princeton University Press, Princeton, New Jersey, pp. 137–148.

Bromage, T. G., R. S. Lacruz, R. Hogg, H. M. Goldman, S. C. McFarlin, J. Warshaw, W. Dirks, A. Perez-Ochoa, I. Smolyar, D. H. Enlow, and A. Boyde. 2009. Lamellar bone is an incremental tissue

reconciling enamel rhythms, body size, and organismal life history. Calcified Tissue International 84:388–404.

Bromage TG, Goldman HM, McFarlin SC J. Warshaw, A. Boyde, and C. M. Riggs. 2003. Circularly polarized light standards for investigations of collagen fiber orientation in bone. *Anatomical record. Part B, New anatomist* **274**, 157–68.

Buffenstein, R, KN Lewis, PA Gibney, V Narayan, KM Grimes, M Smith, TD Lin, HM Brown-Borg. 2020. Probing Pedomorphy and Prolonged Lifespan in Naked Mole-Rats and Dwarf Mice. Physiology, 35:2, 96-111.

Buffenstein R. 2008. Negligible senescence in the longest living rodent, the naked mole-rat: insights from a successfully aging species. J. Comp. Physiol. B, 178, 439–445.

Buffenstein R. 2000. Ecophysiological responses of subterranean rodents to underground habitats. In: Life Underground: The Biology of Subterranean Rodents. (eds Lacey EA, Patton J, Cameron GN), pp. 449, Chicago: The University of Chicago Press.

Buffenstein R. 1996. Ecophysiological responses to a subterranean habitat; a Bathyergid perspective. Mammalia 60, 591–605.

Buffenstein R, Pitcher T. 1996. Calcium homeostasis in mole-rats by manipulation of teeth and bone calcium reservoirs. In: The Comparative Endocrinology of Calcium Regulation. (eds Dacke CG, Danks J, Caple I, Flik G), pp. 220. Bristol: Society for Endocrinology.

Buffenstein R, Laundy M, Pitcher T, J.M. Pettifor. 1995. Vitamin D3 intoxication in naked mole-rats (*Heterocephalus glaber*) leads to hypercalcemia and increased calcium deposition in teeth with evidence of abnormal skin calcification. Gen Comp Endocrinol 99, 35–40.

Buffenstein, R., J. Jarvis, L.A. Opperman, M. Cavaleros, F.P. Ross, J.M. Pettifor. 1994. Subterranean mole-rats naturally have an impoverished calciol status, yet synthesize calciol metabolites and calbindins, Eur. J. Endocrinol. 130, 402–409.

Buffenstein, R., I.N. Sergeev, J.M. Pettifor. 1993. Vitamin D hydroxylases and their regulation in a naturally vitamin D-deficient subterranean mammal, the naked mole rat (*Heterocephalus glaber*), J. Endocrinol. 138 (1993) 59–64.

Buffenstein R, Yahav S. 1991. Is the naked mole-rat, *Heterocephalus glaber*, a poikilothermic or poorly thermoregulating endothermic mammal? *J Therm Biol.* 16:227–232.

Cadet ER, Gafni RI, McCarthy EF, McCray DR, Bacher JD, Barnes KM, Baron J. 2003. Mechanisms responsible for longitudinal growth of the cortex: coalescence of trabecular bone into cortical bone. J Bone Joint Surg Am 85:1737–1748

Calderón, T, D. DeMiguel, W. Arnold, G. Stalder, M. Köhler. 2019. Calibration of life history traits with epiphyseal closure, dental eruption and bone histology in captive and wild red deer J. Anat., 235: 205-216.

Cambra-Moo, O., Nacarino-Meneses, C., Díaz-Güemes, I., Enciso, S., García Gil, O., Llorente Rodríguez, L., Rodríguez Barbero, M.Á., de Aza, A.H., González Martín, A., 2015. Multidisciplinary characterization of the long-bone cortex growth patterns through sheep's ontogeny. J. Struct. Biol. 191, 1–9.

Cambra-Moo, O., Nacarino Meneses, C., Rodríguez Barbero, M.A., García Gil, O., Rascón Pérez, J., Rello Varona, S., D'Angelo, M., Campo Martín, M., González Martín, A., 2014. An approach to the histomorphological and histochemical variations of the humerus cortical bone through human ontogeny. J. Anat. 224 (6), 636–646.

Carmeli-Ligati S, Anna Shipova, Maïtena Dumont, Susanne Holtz, Thomas Hildebrandt, Ron Shahar. 2019 The structure, composition and mechanical properties of the skeleton of the naked mole-rat (*Heterocephalus glaber*). Bone (128), 115035.

Carrier R. 1983. Postnatal ontogeny of the musculo-skeletal system in the Black- tailed jack rabbit (*Lepus californicus*). *Journal of Zoology, London* **201**, 27–55.

Casinos A, Quintana C, Viladiu C. 1993. Allometry and adaptation in the long bones of a digging group of rodents (Ctenomyinae). *Zoological Journal of the Linnean Society* **107**, 107–115.

Castanet J. 2006. Time recording in bone microstructures of endothermic animals; functional relationships. *Comptes Rendus Palevol* **5**, 629–636.

Castanet J, Croci S, Aujard F, M. Perret, J. Cubo, and E. de Margerie. 2004. Lines of arrested growth in bone and age estimation in a small primate: *Microcebus murinus*. *Journal of zoology of london* **263**, 31–39.

Castanet, J., H. Francillon-Vieillot, F. Meunier and A. de Ricqlès. 1993. Bone and individual aging. In: Bone Vol. 7 Bone Growth - B. B. Hall, Ed. CRC Press. Boca Raton, Florida. 353 pp.

Cerroni AM, Tomlinson GA, Turnquist JE, Grynpas MD. 2000. Bone mineral density, osteopenia, and osteoporosis in the rhesus Macaques of Cayo Santiago. American Journal of Physical Anthropology 113: 389–410.

Chinsamy, A, Warburton, NM. 2020. Ontogenetic growth and the development of a unique fibrocartilage entheses in *Macropus fuliginosus*. Zoology (In Press). https://doi.org/10.1016/j.zool.2020.125860

Chinsamy-Turan A. 2012. The microstructure of bones and teeth of nonmammalian therapsids. In: Chinsamy-Turan A, ed. Forerunners of mammals: radiation, histology, biology. Bloomington and Indianapolis: Indiana University Press, 65–88.

Chinsamy A, Hurum J. 2006. Bone microstructure and growth patterns of early mammals. *Acta Palaeontologica Polonica* **51**, 325–338.

Chinsamy-Turan A. 2005. The Microstructure of Dinosaur Bone. Deciphering Biology with Fine-Scale Techniques. Baltimore, Maryland: The Johns Hopkins University Press.

Chinsamy A, Raath M. 1992. Preparation of fossil bone for histological examination. Palaeontologia Africana 29: 39–44.

Currey, M.N. Dean, R. Shahar, 2017. Revisiting the links between bone remodeling and osteocytes: insights from across phyla, Biol. Rev. Camb. Philos. Soc. 92: 1702–1719.

Currey, J., R. Alexander. 1985. The thickness of the walls of tubular bones. Journal of Zoology (A) 206:453–468.

Dammann P, Burda H. 2007. Senescence patterns in African mole-rats (Bathyergidae, Rodentia). In: Begall S, In: Burda H., In: Schleich C, eds. Subterranean Rodents : News from Underground. Heiderberg, Germany : Springer-Verlag, 251-263.

Dengler-Crish C, Catania KC. 2009. Cessation of Reproduction-Related Spine Elongation After Multiple Breeding Cycles in Female Naked Mole-Rats. Anatomical Record (Hoboken) 292: 131–137.

Dengler-Crish CM, Catania KC. 2007. Phenotypic plasticity in female naked mole-rats after removal from reproductive suppression. Journal of Experimental Biology 210: 4351–4358.

Duque G, Watanabe K. 2011. Osteoporosis Research. Animal Models (G Duque and K Watanabe, Eds.). London: Springer London.

Edrey YH, Park TJ, Kang H, Biney A. Buffenstein R. 2011. Endocrine function and neurobiology of the longest-living rodent, the naked molerat. *Exp Gerontol*, 46:116–123.

Enlow DH. 1969. The Bone of Reptiles. In: Biology of the Reptilia Vol. 1 Morphology A (ed C Gans), pp. 373. Academic Press, London.

Enlow DH. 1963. Principles of Bone Remodeling. An Account of Post-natal Growth and Remodeling Processes in Long Bones and the Mandible. Springfield, IL: Charles C. Thomas.

Enlow DH. 1962. A Study of the Post-Natal Growth and Remodeling of Bone. *American Journal of Anatomy* **110**, 79–101.

Enlow D, Brown S. 1958. A comparative histological study of fossil and recent bone tissues. Part III. The Texas Journal of Science 10: 187–230.

Faulkes, CG., N.C. Bennett. 2009. Reproductive skew in African mole-rats: behavioral and physiological mechanisms to maintain high skew. Ch. 13. In Reproductive Skew in Vertebrates: Proximate and Ultimate Causes, ed. Reinmar Hager and Clara B. Jones. Published by Cambridge University Press.

Felder AA, Phillips C, Cornish H, Cooke M, Hutchinson JR, Doube M. 2017. Secondary osteons scale allometrically in mammalian humerus and femur. R Soc Open Sci.;4(11):170431.

Foote J. 1916. A contribution to the comparative histology of the femur (A Hrdlicka, Ed.). Washington: The Smithsonian Institution.

Francillon-Vieillot H, de Buffrénil V, Castanet J. 1990. Microstructures and mineralization of vertebrate skeletal tissues. In: *Skeletal biomineralizations: patterns, processes and evolutionary trends* (ed Carter J), pp. 471–530. Van Nostrand Reinhold, New York.

Frost HM, Jee WS. 1992. On the rat model of human osteopenias and osteoporoses. Bone and Mineral 18, 227–236.

García-Martínez R, Marín-Moratalla N, Jordana X, Köhler, M. 2011. The ontogeny of bone growth in two species of dormice: Reconstructing life history traits. Comptes Rendus Palevol 10, 489–498.

Geiger, M., LAB. Wilson, L. Costeur, R. Sánchez, MR Sánchez-Villagra. 2013. Diversity and body size in giant caviomorphs (Rodentia) from the northern Neotropics—a study of femoral variation. Journal of Vertebrate Paleontology 33:1449–1456.

Gilbert JD, Rossiter SJ, Faulkes CG. 2020. The relationship between individual phenotype and the division of labour in naked mole-rats: it's complicated. PeerJ 8:e9891

Golden NH, Carlson JL. The pathophysiology of amenorrhea in the adolescent. Ann NY Acad Sci 2008;1135:163–78.

Goldman, H. M., S. C. McFarlin, D. M. L. Cooper, C. D. L. Thomas, J. G. Clement. 2009. Ontogenetic patterning of cortical bone microstructure and geometry at the human mid-shaft femur. *Anatomical record* **292**, 48–64.

Goldman, H. M., T. G. Bromage, C. D. L. Thomas, J. G. Clement. 2003. Preferred collagen fiber orientation in the human mid-shaft femur. The anatomical record. Part A 272A, 434–445.

Goldman, B.D., Goldman, S.L., Lanz, T., Magaurin, A., Maurice, A., 1999. Factors influencing metabolic rate in naked mole-rats (*Heterocephalus glaber*). Physiol. Behav. 66, 447–459.

Hall BK. 1978. Developmental and Cellular Skeletal Biology. New York: Academic Press.

Hamar, M. & A. Prodanascu. 1971. Age determination in *Spalax microphthalmus* (Rodentia, Spalacidae). Ann. Zool. Fenn. 8(1): 60-63.

Hart, L., and M. O'Riain. 2006. Is the Cape dune mole-rat, *Bathyergus suillus* (Rodentia: Bathyergidae), a seasonal or aseasonal breeder? Journal of Mammalogy 87: 1078–1085.

Heck CT, Varricchio DJ, Gaudin TJ, Woodward HN, Horner JR. 2019. Ontogenetic changes in the long bone microstructure in the nine-banded armadillo (*Dasypus novemcinctus*). PLoS ONE 14(4): e0215655.

Heinrich RE, Ruff CB, Adamczewski JZ. 1999. Ontogenetic changes in mineralization and bone geometry in the femur of muskoxen (*Ovibos moschatus*). Journal of Zoology, 247: 215–223.

Henry EC, Dengler-Crish CM, Catania KC. 2007. Growing out of a caste--reproduction and the making of the queen mole-rat. Journal of Experimental Biology 210: 261–268.

Hislop, M.S., Buffenstein, R., 1994. Noradrenaline induces nonshivering thermogenesis in both the naked mole-rat (*Heterocephalus glaber*) and the Damara mole-rat (*Cryptomys damarensis*) despite very different modes of thermoregulation. J. Therm. Biol. 19, 25–32.

Holtze, S., Braude, S., Lemma, A., Koch, R., Morhart, M., Szafranski, K., Platzer, M., Alemayehu, F., Goeritz, F., Hildebrandt, T.B., 2018. The microenvironment of naked mole-rat burrows in East Africa. Afr. J. Ecol. 56, 279–289.

Hood, W. R., Kessler, D. S., & Oftedal, O. T. 2014. Milk composition and lactation strategy of a eusocial mammal, the naked mole-rat. Journal of Zoology, 293(2), 108–118.

Hulbert, AJ. 1980. The evolution of energy metabolism in mammals. In Comparative physiology: primitive mammals (Eds. Schmidt-Nielsen et al.). Cambridge University Press. 129-139.

Jarvis JUM., PW. Sherman. 2002. *Heterocephalus glaber.* Mammalian Species, No. 706: 1-9.

Jarvis, JUM. 1991. Reproduction of Naked Mole-rats. In: The Biology of the Naked mole-rat. (Ed. by P.W. Sherman, J.U.M. Jarvis and R.D. Alexander), pp. 384-425. Princeton University Press, Princeton, New Jersey.

Jarvis JUM, O'Riain MJ, McDaid E. 1991. Growth and factors affecting body size in naked mole-rats. in The Biology of the Naked Mole-rat, eds. Sherman, P. W., Jarvis, J. U. M. & Alexander, R. D. (Princeton Univ. Press, Princeton), pp. 258–383.

Jarvis, JUM. 1981. Eusociality in a mammal: Cooperative breeding in naked mole-rat colonies. Science 212:571-573.

Jarvis J, Sale J. 1971. Burrowing and burrow patterns of East African mole-rats *Tachyoryctes*, *Heliophobius* and *Heterocephalus*. Journal of Zoology 163:451–479.

Jordana, X, N. Marín-Moratalla, B. Moncunill-Solèa, C. Nacarino-Menesesa, M. Köhler. 2016. Ontogenetic changes in the histological features of zonal bone tissue of ruminants: a quantitative approach C. R. Palevol., 15 (2016), pp. 255-266

Klevezal GA. 1996. Recording Structures of Mammals. Determination of Age and Reconstruction of Life History. A.A. Balkema, Rotterdam.

Klevezal, G.A. & M.V. Mina. 1973. Factors determining the patterns of annual layers in the dental tissue and bones of mammals. Zhurn. Obshchei Biologii 34(4): 594-605.

Klevezal GA, Kleinberg SE. 1967. Age Determination of Mammals from Annual Layers in Teeth and Bones. Jerusalem, Israel: Translated from Russian by the Israel Program for Scientific Translations.

Kolb C, Scheyer TM, Veitschegger K, et al. 2015. Mammalian bone palaeohistology: a survey and new data with emphasis on island forms. PeerJ 3, e1358.

Köhler M, Marín-Moratalla N, Jordana X, R. Aanes. 2012. Seasonal bone growth and physiology in endotherms shed light on dinosaur physiology. *Nature* **487**, 358–361.

Köhler, M., and S. Moyà-Solà. 2009. Physiological and life history strategies of a fossil large mammal in a resource-limited environment. Proceedings of the National Academy of Sciences of the United States of America, 106:20354–8.

Kronenberg, H. 2003. Developmental regulation of the growth plate. *Nature* 423, 332–336.

Lacey, EA., & PW Sherman. 1991. Social organization of naked mole-rat colonies: evidence for divisions of labor. Pp. 275-336 in The biology of the naked mole-rat (P. W. Sherman, J. U. M. Jarvis, and R. D. Alexander, eds.). Princeton University Press, New Jersey.

Lammers AR, German RZ. 2002. Ontogenetic allometry in the locomotor skeleton of specialized half-bounding mammals. Journal of Zoology, London 258: 485–495.

Leahy, G.D., 1991. Lamellar-zonal bone in fossil mammals: implications for dinosaur and therapsid paleophysiology. J. Vert. Paleont. 11(3), 42A.

Lee, A, Simons, E. 2015. Wing bone laminarity is not an adaptation for torsional resistance in bats. PeerJ 3:e823.

Legendre LJ, Botha-Brink J. 2018. Digging the compromise: investigating the link between limb bone histology and fossoriality in the aardvark (*Orycteropus afer*). PeerJ; 6:e5216.

Locke M. 2004. Structure of long bones in mammals. J Morphol 262, 546–565.

Lovegrove, BG, G. Heldmaier, T. Ruf. 1993. Circadian activity rhythms in colonies of 'blind' Molerats, Cryptomysdamarensis (Bathyergidae), South African Journal of Zoology, 28:1, 46-55.

Lövy M, Šklíba J, Šumbera R. 2013. Spatial and Temporal Activity Patterns of the Free-Living Giant Mole-Rat (*Fukomys mechowii*), the Largest Social Bathyergid. PLoS ONE 8(1): e55357.

McNab, BK. 1966. The metabolism of fossorial rodents: a study of convergence. Ecology 47, 712–733.

Maloney, SK, Fulley, A, Meyer, L.C.R., Kamerman, P.R., Mitchell, G., Mitchell, D., 2011. Minimum core body temperatures in western grey kangaroos decreases as summer advances: a seasonal pattern or a direct response to water, heat or energy supply?. J. Exp. Biol. 214, 1813-1820.

Marín-Moratalla N, Jordana X, Köhler M. 2013. Bone histology as an approach to providing data on certain key life history traits in mammals: implications for conservation biology. Mamm Biol 78, 422–429.

Margerie, E. de, J.-P. Robin, D. Verrier, J. Cubo, R. Groscolas, J. Castanet. 2004. Assessing a relationship between bone microstructure and growth rate: a fluorescent labelling study in the king penguin chick (*Aptenodytes patagonicus*) Journal of Experimental Biology 2004 207: 869-879.

Margerie, E. de, Cubo, J. and Castanet, J. 2002. Bone typology and growth rate: testing and quantifying "Amprino's rule" in the mallard (*Anas platyrhynchos*). C. R. Biol. 325, 221-230.

Mcfarlin SC, Terranova CJ, Zihlman AL, TG. Bromage. 2016. Primary bone microanatomy records developmental aspects of life history in catarrhine primates. *Journal of Human Evolution* **92**, 60–79.

McFarlin, S. 2006. Ontogenetic variation in long bone microstructure in catarrhines and its significance for life history research. Anthropology, The City University of New York, New York, pp.

Montoya-Sanhueza, G. 2020. Functional Anatomy, Osteogenesis and Bone Microstructure of the Appendicular System of African Mole-Rats (Rodentia: Ctenohystrica: Bathyergidae). PhD Thesis. Submitted to the Department of Biological Sciences, University of Cape Town, South Africa. 268 p.

Montoya-Sanhueza, G, Wilson LAB & Chinsamy A. 2019. Postnatal development of the largest subterranean mammal (*Bathyergus suillus*): Morphology, osteogenesis, and modularity of the appendicular skeleton. Developmental Dynamics.

Montoya-Sanhueza G & Chinsamy A. 2018. Cortical bone adaptation and mineral mobilization in the subterranean mammal *Bathyergus suillus* (Rodentia: Bathyergidae): effects of age and sex. PeerJ 6:e4944.

Montoya-Sanhueza, G & A. Chinsamy. 2017. Long bone histology of the subterranean rodent *Bathyergus suillus* (Bathyergidae): ontogenetic pattern of cortical bone thickening. Journal of Anatomy, 230:203-233.

Montoya-Sanhueza, G & Chinsamy A. 2016. Bone microstructure of two highly specialised subterranean rodents: *Bathyergus suillus* and *Heterocephalus glaber* (Bathyergidae). Biennial Conference Palaeontological Society of Southern Africa (PSSA). Abstract book. Stellenbosch, South Africa, 45.

Montoya-Sanhueza, G. 2014. Bone microstructure of the subterranean rodent *Bathyergus suillus* (Rodentia: Bathyergidae). Master's Thesis. Department of Zoology, University of Cape Town, South Africa.

Mora S, Gilsanz V. 2010. Pubertal growth of the male skeleton (Ch 8). In Osteoporosis in Men (Eds. Orwoll, et al.). Academic Press. P 95-103.

Moshkin MP, Novikov EA, Petrovski DV. 2001. Seasonal changes of thermoregulation in the mole vole *Ellobius talpinus*. Physiol Biochem Zool. ;74(6):869-875.

Nacarino-Meneses, X. Jordana, M. Köhler. 2016. First approach to bone histology and skeletochronology of *Equus hemionus*. C. R. Palevol, 15; 1-7.

Oftedal, O. 1980. Milk and mammalian evolution. In Comparative physiology: primitive mammals (Eds. Schmidt-Nielsen et al.). Cambridge University Press. 31-42.

Okrouhlík J, Šumbera R, Gartner B, Schoemann K,Lövy M, Bennett NC. *In Press*. Are southern African solitary mole-rats homeothermic or heterothermic under natural field conditions? Journal of Thermal Biology.

O'Connor TP, Lee A, Jarvis J, Buffenstein R. 2002. Prolonged longevity in naked mole-rats: age-related changes in metabolism, body composition and gastrointestinal function. Comparative Biochemistry and Physiology. Part A, Molecular & Integrative Physiology, 133(3), 835–42.

O'Riain MJ, Jarvis J, Alexander R, Buffenstein R, Peeters C. 2000. Morphological castes in a vertebrate. Proceedings of the National Academy of Sciences of the United States of America 97:13194–7.

O'Riain MJ, Jarvis JUM. 1998. The dynamics of growth in naked mole-rats: the effects of litter order and changes in social structure. J Zool (Lond) 246: 49– 60, 1998.

O'Riain, M. J. 1996. Pup Ontogeny and Factors Influencing Behavioural and Morphological Variation in Naked Mole-Rats, *Heterocephalus glaber* (Rodentia, Bathyergidae). University of Cape Town.

Orlandi-Oliveras, G., Jordana, X., Moncunill-Sole, B., K€ohler, M., 2016. Bone histology of the giant fossil dormouse *Hypnomys onicensis* (Gliridae, Rodentia) from Balearic Islands. Comptes Rendus Palevol 15, 247e253.

Park, T.J., Reznick, J., Peterson, B.L., Blass, G., Omerbašić, D., Bennett, N.C., Kuich, P H J L, Zasada, C., Browe, B.M., Hamann, W. 2017. Fructose-driven glycolysis supports anoxia resistance in the naked mole-rat. Science 356, 307–311.

Pazzaglia UE, Sibilia V, Congiu T, Pagani F, Ravanelli M, Zarattini G. 2015. Setup of a Bone Aging Experimental Model in the Rabbit Comparing Changes in Cortical and Trabecular Bone: Morphological and Morphometric Study in the Femur. Journal of Morphology 276: 733–747.

Pinto, M., K. J. Jepsen, C. J. Terranova, R. Buffenstein. 2010. Lack of sexual dimorphism in femora of the eusocial and hypogonadic naked mole-rat: A novel animal model for the study of delayed puberty on the skeletal system. *Bone*, 46:112–120.

Pitcher T, Buffenstein R, Keegan JD, GP Moodley, Yahav S. 1992. Dietary calcium content, calcium balance and mode of uptake in a subterranean mammal, the damara mole-rat. J Nutr 122, 108–114.

Pitcher T, Pettifor JM, Buffenstein R. 1994. The effect of dietary calcium content and oral vitamin D3 supplementation on mineral homeostasis in a subterranean mole-rat *Cryptomys damarensis*. Bone Miner 27, 145–157.

Prendergast BJ, Renstrom RA, Nelson RJ. 2004. Genetic Analyses of a Seasonal Interval Timer. Journal of Biological Rhythms, 19(4): 298-311.

Puzachenko, A.Yu. 1991. Age determination of *Spalax microphthalmus* (Rodentia, Spalacidae). Zool. Zhurn. 70(12): 113-124.

Ratajczak HV, PT Thomas, RB Sothern, T Vollmuth, JD Heck. 1993. Evidence for Genetic Basis of Seasonal Differences in Antibody Formation Between Two Mouse Strains. Chronobiology International, 10:5, 383-394

Reid, R.E.H., 1996. Bone histology of the Cleveland-Lloyd dinosaurs and of dinosaurs 541 in general, Part I, Introduction: Introduction to bone tissues. Brigham Young 542 University Geology Studies, 41, 25–72.

Riccio, A.P., Goldman, B.D., 2000. Circadian rhythms of body temperature and metabolic rate in naked mole-rats. Physiol. Behav. 71, 15–22.

Ricqlès A de, Meunier FJ, Castanet J, Francillon-Vieillot H. 1991. Comparative microstructure of bone. In: Hall BK, ed. Bone Matrix and Bone Specific Products. Boca Raton: CRC Press, 1–78.

Ruby, JG, M Smith, R Buffenstein. 2018. Naked mole-rat mortality rates defy Gompertzian laws by not increasing with age. eLife 7:e31157.

Ruth EB. 1953. Bone studies. II. An experimental study of the haversian-type vascular channels. The American Journal of Anatomy 93: 429–455.

Samuels JX, Valkenburgh B Van. 2008. Skeletal Indicators of Locomotor Adaptations in Living and Extinct Rodents. Journal of Morphology 269: 1387–1411.

Sanger TJ, Norgard EA, Pletscher LS, Bevilacqua M, Brooks VR, Sandell LJ, Cheverud JM. 2011. Developmental and Genetic Origins of Murine Long Bone Length Variation. Journal of Experimental Zoology. Part B, Molecular and Developmental Evolution 316: 146–161.

Seeman, E. 2002. Pathogenesis of bone fragility in women and men, Lancet 359, 1841–1850.

Seeman, E. 2001. Clinical review 137: sexual dimorphism in skeletal size, density, and strength, J. Clin. Endocrinol. Metab. 86 (10), 4576–4584.

Silva MJ, Jepsen KJ. 2013. Age related changes in whole-bone structure and strength. In: Silva MJ, ed. Skeletal Aging and Osteoporosis. Biomechanics and Mechanobiology. London: Springer Berlin Heidelberg, 1–30.

Singh, I.J., Tonna, E.A., Gandel, C.P., 1974. A comparative histological study of mammalian bone. J. Morph. 144, 421-437.

Sherman PW, Jarvis JUM. 2002. Extraordinary life spans of naked mole-rats (*Heterocephalus glaber*). Journal of Zoology 258: 307–311.

Skinner DC, Moodley G, Buffenstein R. 1991. Is vitamin D3 essential for mineral metabolism in the Damara mole-rat (*Cryptomys damarensis*)? Gen Comp Endocrinol 81, 500–505.

Skulachev VP, Holtze S, Vyssokikh MY, Bakeeva LE, Skulachev MV, Markov AV, Hildebrandt TB, Sadovnichii VA. 2017. Neoteny, Prolongation of Youth: From Naked Mole Rats to "Naked Apes" (Humans). Physiol Rev 97: 699–720.

Smith, CCD., 2020. *Giraffa camelopardalis*: Limb Bone Histology Through Ontogeny. Masters dissertation, University of Cape Town.

Smith JW. 1960. Collagen fibre patterns in mammalian bone. *Journal of anatomy* **94**, 329–344.

Starck, J.M., Chinsamy, A., 2002. Bone microstructure and developmental plasticity in birds and other dinosaurs. J. Morph. 254, 232-246.

Straehl FR, Scheyer TM, Forasiepi AM, MacPhee RD, Sánchez-Villagra MR. 2013. Evolutionary patterns of bone histology and bone compactness in xenarthran mammal long bones. *PloS one* **8**, e69275.

Streicher S, Boyles JG, Oosthuizen MK, Bennett NC. 2011. Body Temperature Patterns and Rhythmicity in Free-Ranging Subterranean Damaraland Mole-Rats, *Fukomys damarensis*. PLoS ONE 6(10): e26346.

Šumbera, 2019. Thermal biology of a strictly subterranean mammalian family, the African mole-rats (Bathyergidae, Rodentia) - a review. *Journal of Thermal Biology*, 79:166-189.

Šumbera, R., Chitaukali, W.N., Elichová, M., Kubová, J., Burda, H., 2004. Microclimatic stability in burrows of an Afrotropical solitary bathyergid rodent, the silvery mole-rat (*Heliophobius argenteocinereus*). J. Zool. 263, 409–416.

Tian J, Azpurua C, Hine A, Vaidya M, Myakishev-Rempel J, Ablaeva Z, Mao E, Nevo V, Gorbunova A, Seluanov. 2013. High-molecular-mass hyaluronan mediates the Cancer resistance of the naked mole rat. Nature 499:346–349.

Tucker, R. 1981. The digging behavior and skin differentiations in *Heterocephalus glaber*. J. Morphol., 168: 51-71.

Urison, N., Buffenstein, R., 1995. Metabolic and body temperature changes during pregnancy and lactation in the naked mole-rat (*Heterocephalus glaber*). Physiol. Zool. 68, 402–420.

Urison, N.T., Buffenstein, R. 1994. Shifts in thermoregulatory patterns with pregnancy in the poikilothermic mammal - the naked mole-rat (*Heterocephalus glaber*). J. Therm. Biol. 19, 365–371.

Wall, WP. 1983. The Correlation between High Limb-Bone Density and Aquatic Habits in Recent Mammals. Journal of Paleontology 57:197–207.

Walker, M.M., Louys, J., Herries, A.I.R., Gilbert, J.P., Miszkiewicz, J.J., 2020. Humerus midshaft histology in a modern and fossil wombat. Aust. Mamm. https://doi.org/10.1071/AM20005

Warshaw J. 2008. Comparative primate bone microstructure: records of life history, function, and phylogeny. In: Mammalian Evolutionary Morphology. A Tribute to Frederick S. Szalay (Eds E Sargis, M Dagosto), pp. 440. Vertebrate Paleobiology and Paleoanthropology Series, Springer.

Werning, SA. 2013 (a). Evolution of Bone Histological Characters in Amniotes, and the Implications for the Evolution of Growth and Metabolism. PhD dissertation. University of California, Berkeley.

Werning, SA. 2013 (b). Osteohistological differences between marsupials and placental mammals reflect both growth rates and life history strategies. Abstract. Society for Integrative and Comparative Biology.

Webber, T, Patel, SP, Pensak, M, Fajolu, O, Rozental, TD, Wolf, JM. 2015. Correlation Between Distal Radial Cortical Thickness and Bone Mineral Density. Journal of Hand Surgery, Vol: 40(3): 493-499.

Wongdee, K., Krishnamra, N. Charoenphandhu, N. 2012. Endochondral bone growth, bone calcium accretion, and bone mineral density: how are they related?. *J Physiol Sci* 62, 299–307.

Woodley, R, R. Buffenstein. 2002. Thermogenic changes with chronic cold exposure in the naked mole-rat (*Heterocephalus glaber*). Comparative Biochemistry and Physiology Part A 133: 827–834.

Yingling VR, Taylor G. 2008. Delayed pubertal development by hypothalamic suppression causes an increase in periosteal modeling but a reduction in bone strength in growing female rats. Bone 42: 1137–1143.

Young JW, Fernandez D, Fleagle JG. 2010. Ontogeny of long bone geometry in capuchin monkeys (*Cebus albifrons* and *Cebus apella*): implications for locomotor development and life history. Biology Letters 6: 197–200.

Zelová, J., Šumbera, R., Okrouhlík, J., Šklíba, J., Lövy, M., Burda, H., 2011. A seasonal difference of daily energy expenditure in a free-living subterranean rodent, the silvery mole-rat (*Heliophobius argenteocinereus*; Bathyergidae). Comp. Biochem. Physiol. -Part Mol. Integr. Physiol. 158, 17–21.

Zelová, J., Šumbera, R., Sedláček, F., Burda, H., 2007. Energetics in a solitary subterranean rodent, the silvery mole-rat, *Heliophobius argenteocinereus* and allometry of RMR in African mole-rats (Bathyergidae). Comp. Biochem. Physiol. -Mol. Integr. Physiol. 147, 412–419.

Figure 1. Periosteal ossification during early ontogeny of naked mole-rats (femoral diaphysis of a pup, #010). A) Bone cross-section showing thin cortical walls and a large medullary cavity (MC). Appositional (+) and resorptive (-) surfaces are also indicated. B) External morphology of the diaphysis showing the more even –periosteal– surface of the anterior side and the rougher surface of the posterior side. Periosteal vascular canals (PVC) appear forming part of the mineralizing front in the posterior side of the bone, close where the nutrient foramen (NF) develops. C) Detail of the endosteal surface showing Howship's

lacunae (HL) indicating resorptive activity associated with the expansion of the MC. See abbreviations in the text.

Figure 2. Histomorphogenesis of the humerus of naked mole-rats. A) Bone microanatomy of pups (top, #010) and a small juvenile (bottom, #046), showing differences in bone size. B) Large juveniles (#067 and #045) showing cortical thickening. C) A large adult (#008) with thick cortical walls and elongated cross-sectional shape. D) Anterolateral side of a juvenile showing the development of resorption cavities (RC), which results in trabecularized bone (TrB). E) Lateral and F) medial sides showing thin cortical walls composed of woven (WB), parallel-fibered bone (PFB) and lamellar bone (LB). A resorption line (RL) also appears in the intracortical region. G) Anterolateral side of juvenile (#002) showing secondary reconstruction in TrB and formation of annuli (arrow heads) in endocortical regions. H) Posterior side of juvenile (#067) showing intact areas of bone deposition of mainly endosteal origin, as well as double RLs and a band of WB indicating changes in the direction of the osteogenesis. PFB and lamellar-zonal bone (LZB) are also observed in the cortex. I) Anterolateral sides of an adult (#008) showing increased resorptive activity and trabecularization. J) Same adult showing mixture of bone matrices and decreased rates of osteogenesis in the pericortical region of the posterior side. K) Secondary osteon in posteromedial side of an adult (#501). See abbreviations in the text.

Figure 3. Histomorphogenesis of the ulna of naked mole-rats. A) Bone microstructure of the pup (top, #010), juveniles (#046, #067, #088) and adults (#008) showing differences in cross-sectional shape, size and cortical thickening. B) Small (#046) and large (#088) juveniles and a large adult (#008) showing periosteal bone apposition in the anterior side, as well as formation of LAGs (arrow heads) in adulthood. C) Posterior regions of a large juvenile (#088) and an adult (#008), showing thick cortical walls, mostly composed of woven (WB) and lamellar bone (LB). A thin band of WB surrounded by two resorption lines (RLs) is observed in the intracortical region and indicates changes in the direction of the osteogenesis during ontogeny. See abbreviations in the text.

Figure 4. Histomorphogenesis of the femur of naked mole-rats. A) Bone microanatomy of a pup (top, #010) and a small juvenile (bottom, #046) showing differences in bone size. B) Large juveniles (#088 and #045) showing cortical thickening and variation in bone shape, cortical thickness and medullary cavity (MC) size. C) Adult (#008) showing a larger bone with thick cortical walls and elongated cross-sectional shape. D) Lateral, E) anterior and F)

posterior sides of juvenile showing thin cortical walls. G) Lateral side of juvenile (#088) showing the tip of the femur associated with the distal origin of the third trochanter (dTt). This region is composed of periosteal lamellar bone (PLB), suggesting slower growth rates as compared to other regions of the bone. H) Posteromedial side of same juvenile showing stratified deposition of parallel-fibered bone (PFB) and annuli of lamellar bone (LB) (arrow-heads). In the posterior side, the pericortical region also showed LB. I) Half section of a large juvenile showing the posterior side with multiple stratified bone matrices with LB annuli (arrow-heads). A change in the direction and rate of osteogenesis is observed in the intracortical region, which is delimited by a resorption line (RL). The periosteal region showed more slowly deposited tissues (e.g. PLB). J) Lateral, K) anteromedial and L) posteromedial sides of a large adult (#008) showing increased cortical thicknesses, abundant lacunae and PLB. Some longitudinal and radial vascularization is observed in the anteromedial region (K), as well as formation of PLB (L). See abbreviations in the text.

Figure 5. Histomorphogenesis of the tibia of naked mole-rats. A) Bone microanatomy of a pup (#010), a small juvenile (#046) and an adult (#008) showing main differences in bone size, shape and cortical thickness. B) Anterior and C) posterior sides of a large juvenile (#067) showing cortical thickening and formation of zonal bone. Arrow-heads indicate annuli of lamellar bone (LB) that appeared around the entire cross-section. Juveniles already show slowly deposited bone tissues such as periosteal lamellar bone (PLB) in the pericortical region. D) Anterior and E) posterior sides of a large adult (#008) showing considerable cortical thickening, mostly by parallel-fibered (PFB) and PLB. The anterior side shows endocortical and pericortical regions composed of LB delimited by double resorption lines (RLs), with an intracortical region of PFB, indicating changes in the rates of osteogenesis during ontogeny. See abbreviations in the text.

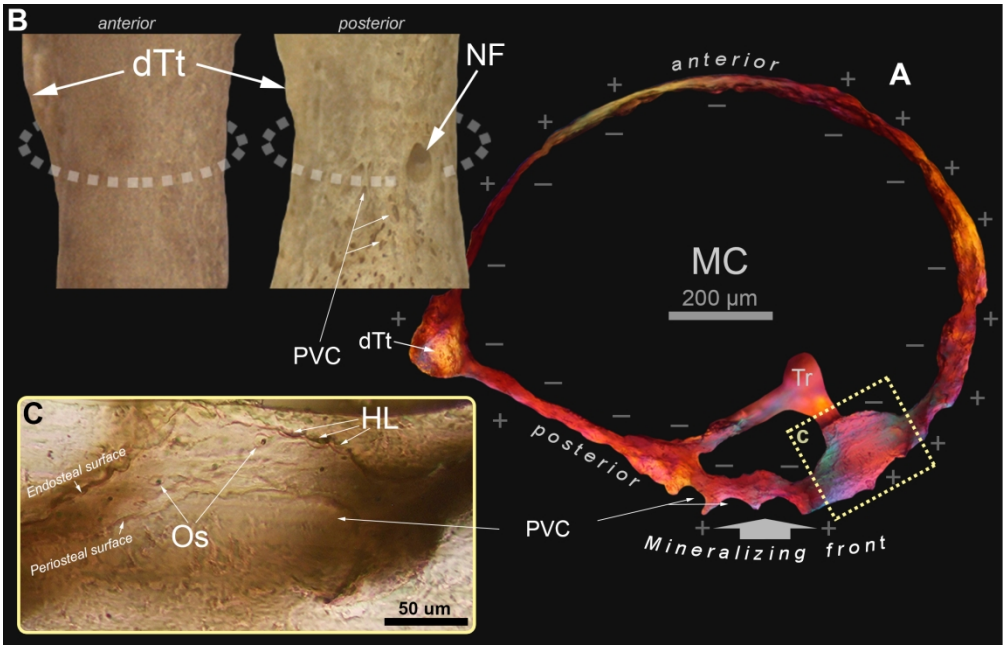

Figure 1. Periosteal ossification during early ontogeny of naked mole-rats (femoral diaphysis of a pup, #010). A) Bone cross-section showing thin cortical walls and a large medullary cavity (MC). Appositional (+) and resorptive (-) surfaces are also indicated. B) External morphology of the diaphysis showing the more even –periosteal– surface of the anterior side and the rougher surface of the posterior side. Periosteal vascular canals (PVC) appear forming part of the mineralizing front in the posterior side of the bone, close where the nutrient foramen (NF) develops. C) Detail of the endosteal surface showing Howship's lacunae (HL) indicating resorptive activity associated with the expansion of the MC. See abbreviations in the text.

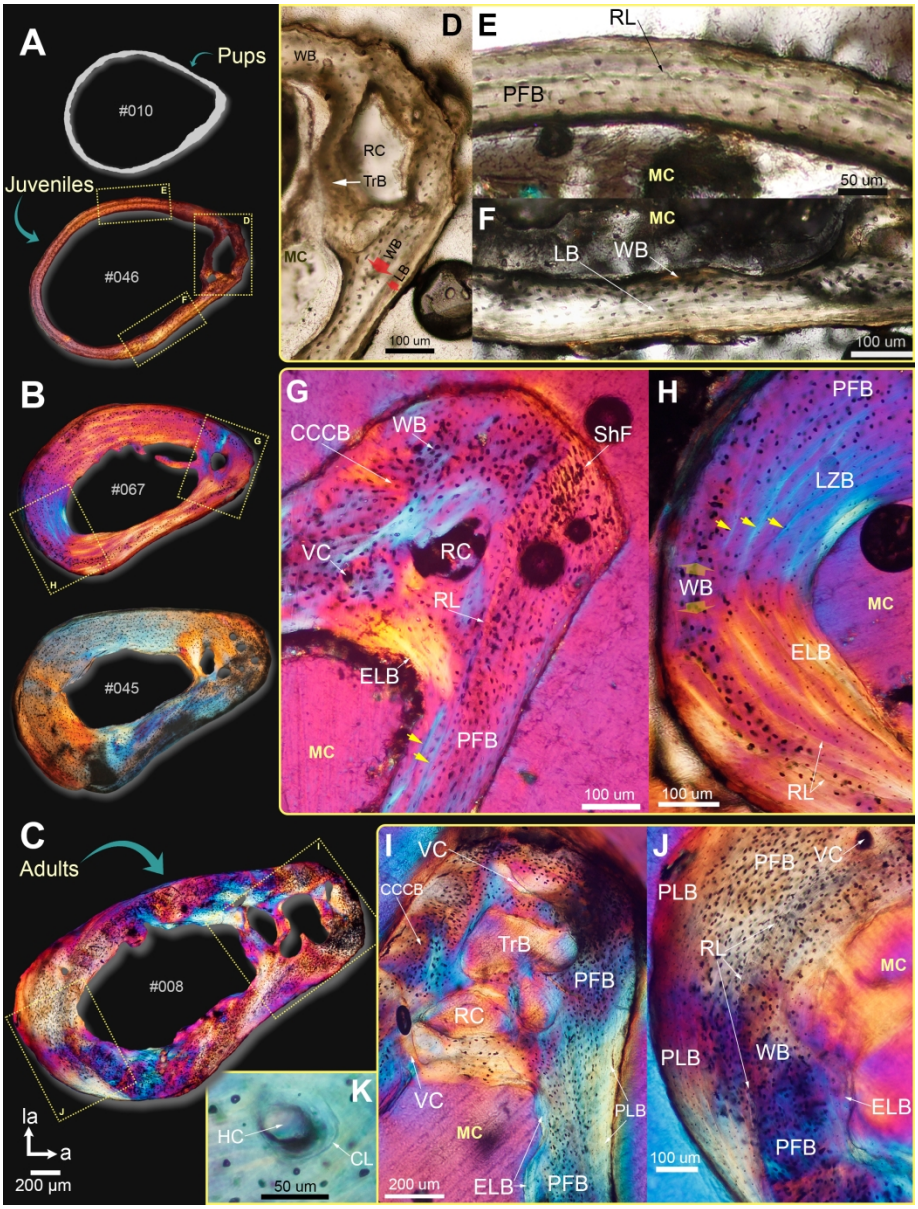

Figure 2. Histomorphogenesis of the humerus of naked mole-rats. A) Bone microanatomy of pups (top, #010) and a small juvenile (bottom, #046), showing differences in bone size. B) Large juveniles (#067 and #045) showing cortical thickening. C) A large adult (#008) with thick cortical walls and elongated cross-sectional shape. D) Anterolateral side of a juvenile showing the development of resorption cavities (RC), which results in trabecularized bone (TrB). E) Lateral and F) medial sides showing thin cortical walls composed of woven (WB), parallel-fibered bone (PFB) and lamellar bone (LB). A resorption line (RL) also appears in the intracortical region. G) Anterolateral side of juvenile (#002) showing secondary reconstruction in TrB and formation of annuli (arrow heads) in endocortical regions. H) Posterior side of juvenile (#067) showing intact areas of bone deposition of mainly endosteal origin, as well as double RLs and a band of WB indicating changes in the direction of the osteogenesis. PFB and lamellar-zonal bone (LZB) are also observed in the cortex. I) Anterolateral sides of an adult (#008) showing increased resorptive activity and trabecularization. J) Same adult showing mixture of bone matrices and decreased rates of osteogenesis in the pericortical region of the posterior side. K) Secondary osteon in posteromedial side of an adult (#501). See abbreviations in the text.

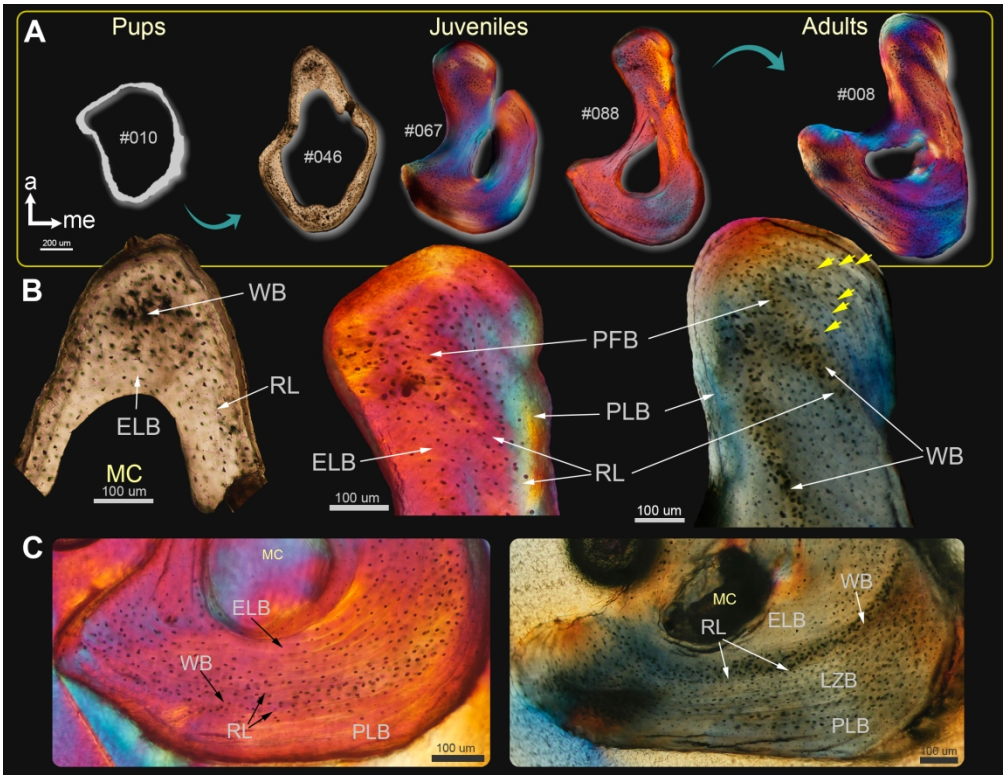

Figure 3. Histomorphogenesis of the ulna of naked mole-rats. A) Bone microstructure of the pup (top, #010), juveniles (#046, #067, #088) and adults (#008) showing differences in cross-sectional shape, size and cortical thickening. B) Small (#046) and large (#088) juveniles and a large adult (#008) showing periosteal bone apposition in the anterior side, as well as formation of LAGs (arrow heads) in adulthood. C) Posterior regions of a large juvenile (#088) and an adult (#008), showing thick cortical walls, mostly composed of woven (WB) and lamellar bone (LB). A thin band of WB surrounded by two resorption lines (RLs) is observed in the intracortical region and indicates changes in the direction of the osteogenesis during ontogeny. See abbreviations in the text.

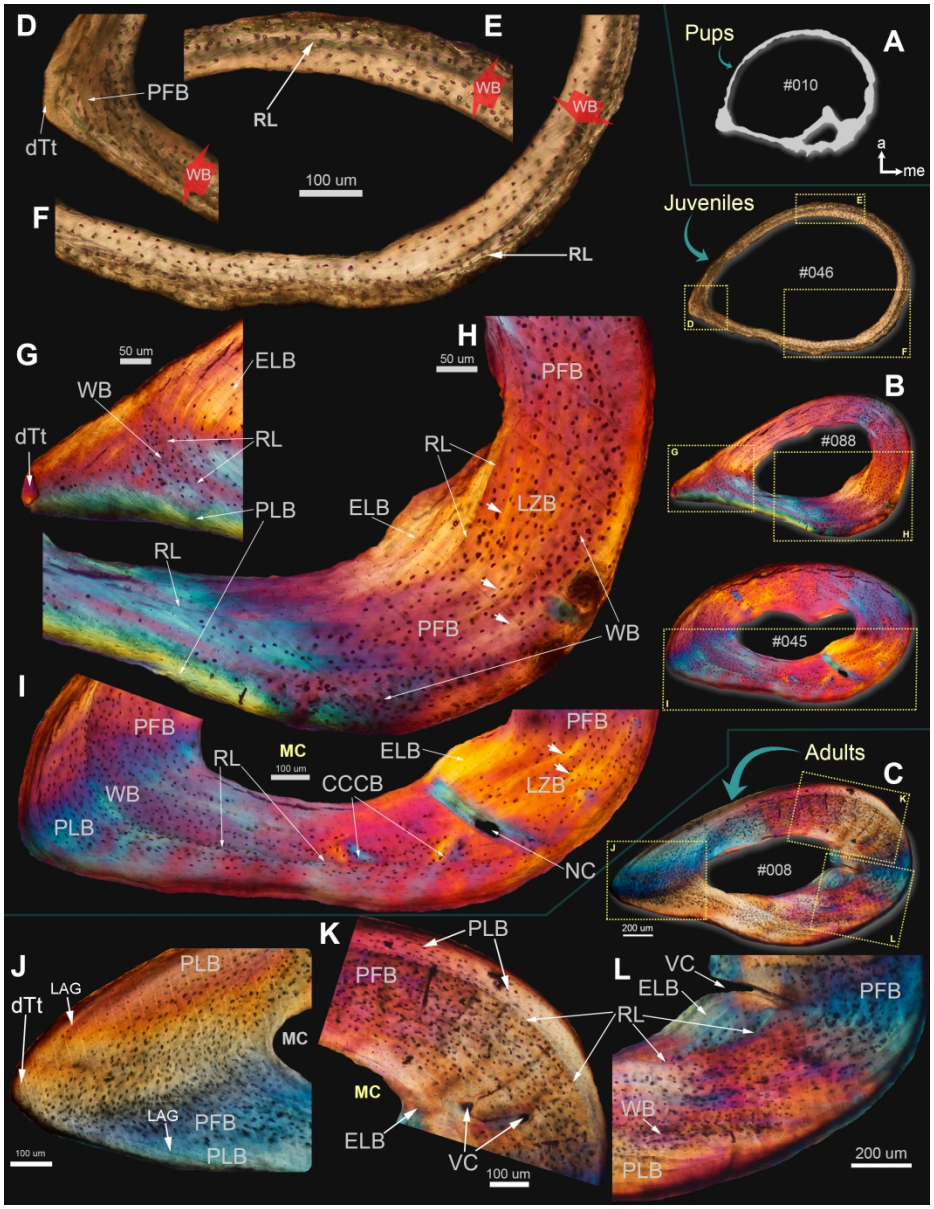

Figure 4. Histomorphogenesis of the femur of naked mole-rats. A) Bone microanatomy of a pup (top, #010) and a small juvenile (bottom, #046) showing differences in bone size. B) Large juveniles (#088 and #045) showing cortical thickening and variation in bone shape, cortical thickness and medullary cavity (MC) size. C) Adult (#008) showing a larger bone with thick cortical walls and elongated cross-sectional shape. D) Lateral, E) anterior and F) posterior sides of juvenile showing thin cortical walls. G) Lateral side of juvenile (#088) showing the tip of the femur associated with the distal origin of the third trochanter (dTt). This region is composed of periosteal lamellar bone (PLB), suggesting slower growth rates as compared to other regions of the bone. H) Posteromedial side of same juvenile showing stratified deposition of parallel-fibered bone (PFB) and annuli of lamellar bone (LB) (arrow-heads). In the posterior side, the pericortical region also showed LB. I) Half section of a large juvenile showing the posterior side with multiple stratified bone matrices with LB annuli (arrow-heads). A change in the direction and rate of osteogenesis is observed in the intracortical region, which is delimited by a resorption line (RL). The periosteal region showed more slowly deposited tissues (e.g. PLB). J) Lateral, K) anteromedial and L) posteromedial sides of a large adult (#008) showing increased cortical thicknesses, abundant lacunae and PLB. Some longitudinal and radial

vascularization is observed in the anteromedial region (K), as well as formation of PLB (L). See abbreviations in the text.

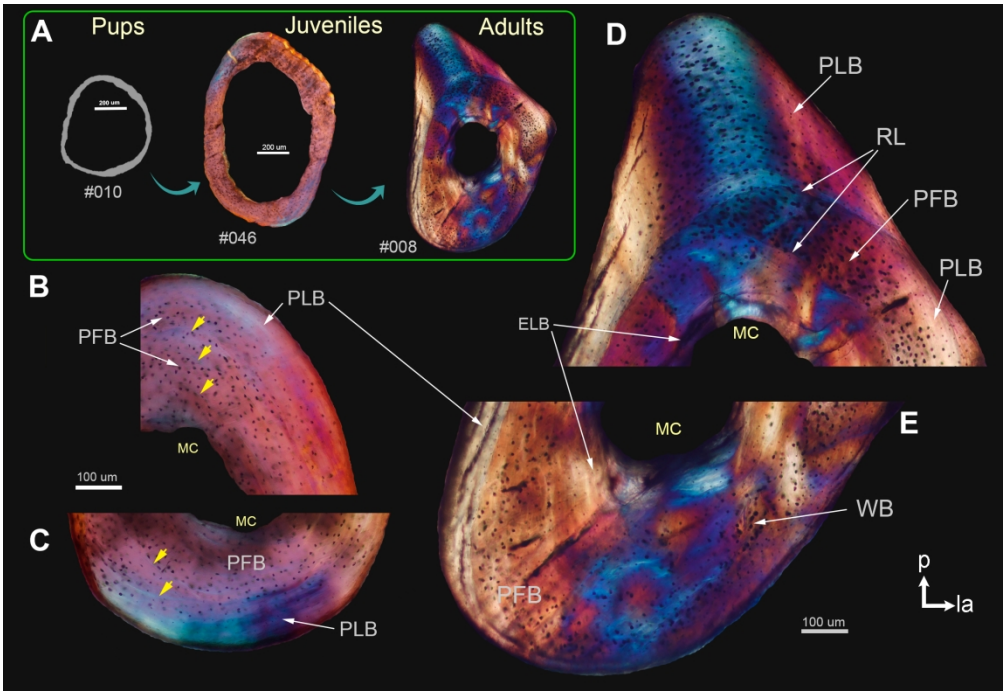

Figure 5. Histomorphogenesis of the tibia of naked mole-rats. A) Bone microanatomy of a pup (#010), a small juvenile (#046) and an adult (#008) showing main differences in bone size, shape and cortical thickness. B) Anterior and C) posterior sides of a large juvenile (#067) showing cortical thickening and formation of zonal bone. Arrow-heads indicate annuli of lamellar bone (LB) that appeared around the entire cross-section. Juveniles already show slowly deposited bone tissues such as periosteal lamellar bone (PLB) in the pericortical region. D) Anterior and E) posterior sides of a large adult (#008) showing considerable cortical thickening, mostly by parallel-fibered (PFB) and PLB. The anterior side shows endocortical and pericortical regions composed of LB delimited by double resorption lines (RLs), with an intracortical region of PFB, indicating changes in the rates of osteogenesis during ontogeny. See abbreviations in the text.

ID GM	Institution	Sex	Age (years)	Molar eruption	Tooth wear	Relative age
JJ-001	UCT	F	1.5	3/3	Infolding	Juvenile
JJ-002	UCT	-	-	3/3	Infolding	Juvenile
JJ-008	UCT	F	~10	3/3	Enamel ring	Adult
JJ-009	UCT	M	-	3/3	Enamel ring	Adult
JJ-010	UCT	-	0.33	2/2	Cuspids	Pup
JJ-045	UCT	M	-	3/3	Infolding	Juvenile
JJ-046	UCT	F	-	3/3	Infolding	Juvenile
1200-047	UCT	-	-	3/3	Infolding	Juvenile
1200-048	UCT	M	-	3/3	Enamel ring	Adult
1200-049	UCT	F	-	3/3	Enamel ring	Adult
1200-052	UCT	M	-	3/3	Enamel ring	Adult
1200-053	UCT	M	-	3/3	Enamel ring	Adult
1200-054	UCT	F	-	3/3	Enamel ring	Adult
1200-055	UCT	M	-	3/3	Enamel ring	Adult
1200-056	UCT	-	-	3/3	Enamel ring	Adult
1200-057	UCT	M	-	3/3	Enamel ring	Adult
1200-058	UCT	M	-	3/3	Enamel ring	Adult
1200-059	UCT	F	-	3/3	Enamel ring	Adult
1200-060	UCT	M	-	3/3	Enamel ring	Adult
1200-061	UCT	M	-	3/3	Enamel ring	Adult
1200-063	UCT	F	-	3/3	Enamel ring	Adult
1200-064	UCT	F	-	3/3	Enamel ring	Adult
1200-065	UCT	F	-	3/3	Enamel ring	Adult
1200-066	UCT	-	-	3/3	Infolding	Juvenile
1200-067	UCT	F	-	3/3	Infolding	Juvenile
1200-068	UCT	F	-	3/3	Enamel ring	Adult
1200-069	UCT	-	-	3/3	Infolding	Juvenile
1000-070	UCT	F	-	3/3	Enamel ring	Adult
1000-071	UCT	F	-	3/3	Enamel ring	Adult
1000-073	UCT	M	-	3/3	Enamel ring	Adult
1000-074	UCT	M	-	3/3	Enamel ring	Adult
1000-075	UCT	-	-	3/3	Enamel ring	Adult
1000-076	UCT	F	-	3/3	Enamel ring	Adult
1000-077	UCT	F	-	3/3	Enamel ring	Adult
1000-078	UCT	F	-	3/3	Enamel ring	Adult
1000-079	UCT	F	-	3/3	Enamel ring	Adult
1000-080	UCT	F	-	3/3	Enamel ring	Adult
1000-081	UCT	M	-	3/3	Enamel ring	Adult
1000-082	UCT	M	-	3/3	Enamel ring	Adult
1000-083	UCT	F	-	3/3	Enamel ring	Adult
1000-084	UCT	F	-	3/3	Enamel ring	Adult
1000-085	UCT	M	-	3/3	Enamel ring	Adult
1000-086	UCT	F	-	3/3	Enamel ring	Adult
5000-087	UCT	M	-	3/3	Enamel ring	Adult
5000-088	UCT	M	-	3/3	Infolding	Juvenile
5000-090	UCT	F	-	3/3	Enamel ring	Adult
5000-091	UCT	F	-	3/3	Enamel ring	Adult
5000-092	UCT	M	-	3/3	Enamel ring	Adult
5000-093	UCT	F	-	3/3	Enamel ring	Adult

5000-094	UCT	M	-	3/3	Enamel ring	Adult
5000-095	UCT	M	-	3/3	Infolding	Juvenile
5000-096	UCT	F	-	3/3	Enamel ring	Adult
5000-097	UCT	F	-	3/3	Enamel ring	Adult
5000-098	UCT	F	-	3/3	Enamel ring	Adult
5000-099	UCT	M	-	3/3	Enamel ring	Adult
5000-100	UCT	F	-	2?/3	Enamel ring	Adult
5000-101	UCT	M	-	3/3	Enamel ring	Adult
NB-420	UP	M	-	-	-	-
NB-499	UP	M	-	-	-	-
NB-500	UP	-	-	-	-	-
NB-501	UP	F	-	-	-	-
NB-505	UP	M	-	-	-	-
NB-507	UP	F	-	-	-	-
NB-508	UP	F	-	-	-	-
NB-509	UP	F	-	-	-	-
NB-510	UP	F	-	-	-	-
NB-511	UP	F	-	-	-	-
CDC-156	NOMU	M	2.67	-	-	Adult
CDC-157	NOMU	M	2.67	-	-	Adult
CDC-158	NOMU	M	2.50	-	-	Adult
CDC-159	NOMU	M	2.83	-	-	Adult
CDC-160	NOMU	M	2.75	-	-	Adult
CDC-161	NOMU	M	2.17	-	-	Adult
CDC-162	NOMU	M	2.67	-	-	Adult
CDC-163	NOMU	M	2.33	-	-	Adult
CDC-164	NOMU	M	2.33	-	-	Adult

Table 1. Data of the individuals analyzed in this study: institution of origin, ID, sex, age, relative age and dental information. The molar eruption category indicates number of molars erupted in upper and lower check tooth. Abbreviations: University of Cape Town (UCT); University of Pretoria (UP); Northeast Ohio Medical University (NOMU).